

# Explanation as a Watermark: Towards Harmless and Multi-bit Model Ownership Verification via Watermarking Feature Attribution

Shuo Shao, Yiming Li, Hongwei Yao, Yiling He, Zhan Qin, Kui Ren

State Key Laboratory of Blockchain and Data Security, Zhejiang University

{shaoshuo\_ss, yhongwei, yilinghe, qinzhan, kuiren}@zju.edu.cn; liyiming.tech@gmail.com

**Abstract**—Ownership verification is currently the most critical and widely adopted post-hoc method to safeguard model copyright. In general, model owners exploit it to identify whether a given suspicious third-party model is stolen from them by examining whether it has particular properties ‘inherited’ from their released models. Currently, backdoor-based model watermarks are the primary and cutting-edge methods to implant such properties in the released models. However, backdoor-based methods have two fatal drawbacks, including *harmfulness* and *ambiguity*. The former indicates that they introduce maliciously controllable misclassification behaviors (*i.e.*, backdoor) to the watermarked released models. The latter denotes that malicious users can easily pass the verification by finding other misclassified samples, leading to ownership ambiguity.

In this paper, we argue that both limitations stem from the ‘zero-bit’ nature of existing watermarking schemes, where they exploit the status (*i.e.*, misclassified) of predictions for verification. Motivated by this understanding, we design a new watermarking paradigm, *i.e.*, Explanation as a Watermark (EaaW), that implants verification behaviors into the explanation of feature attribution instead of model predictions. Specifically, EaaW embeds a ‘multi-bit’ watermark into the feature attribution explanation of specific trigger samples without changing the original prediction. We correspondingly design the watermark embedding and extraction algorithms inspired by explainable artificial intelligence. In particular, our approach can be used for different tasks (*e.g.*, image classification and text generation). Extensive experiments verify the effectiveness and harmlessness of our EaaW and its resistance to potential attacks.

## I. INTRODUCTION

In the past few years, Deep Learning (DL) has made significant advancements around the world. The DL model has emerged as a de facto standard model and a pivotal component in various domains and real-world systems, such as computer vision [8], [17], natural language processing [2], [52], and recommendation systems [40], [59]. However, developing high-performance DL models requires substantial amounts of data, human expertise, and computational resources. Accordingly, these models are important intellectual property for their owners and their copyright deserves protection.

Ownership verification is currently the most critical and widely adopted method to safeguard model copyright. Specifically, it intends to identify whether a given suspicious third-party model is an unauthorized copy from model owners. Implanting owner-specified watermarks (*i.e.*, model watermarks) into the (victim) model is the primary solution for ownership verification [50]. Model watermarking methods generally

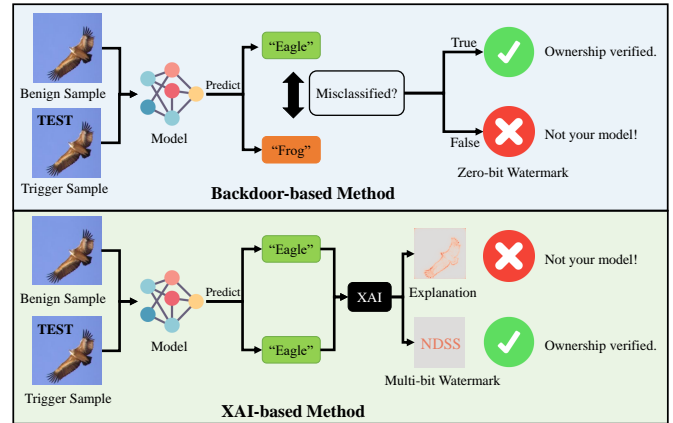


Fig. 1: The main pipeline of our EaaW and backdoor-based methods. Backdoor-based methods depend on the misclassification to determine the ownership. Instead of changing the predictions, our EaaW implants the watermark into the explanation of feature attribution for verification.

have two main stages, including watermark embedding and ownership verification. In the first stage, model owners should embed a specific secret pattern (*i.e.*, watermark) that will be ‘inherited’ by unauthorized model copies into the model. After that, in cases where adversaries may illegally steal the victim model, the model owner can turn to a trusted authority for verification by examining whether the suspicious model has a similar watermark to the one implanted in the victim model. If this watermark is present, the suspect model is an unauthorized version of the victim model.

In real-world applications, DL models are usually used in a black-box manner (*e.g.*, deep learning as a service), where users can only access the model through its API without access to its source files or intermediate results (*e.g.*, gradients). In these scenarios, model owners and verifiers can only exploit the predictions of the suspicious model to conduct the watermark extraction process and the following ownership verification. It is called *black-box ownership verification*, which is the most classical and practical [50].

In the aforementioned black-box scenarios, currently, most of the black-box model watermarking methods [1], [20], [60] are based on backdoor attack [27]. Specifically, the model owners attach an owner-specified unique trigger pattern (*e.g.*, ‘TEST’ sign) to some benign samples from the original dataset while changing their labels to generate trigger samples. Model

owners will use these trigger samples associated with the remaining benign ones to train the victim model. Accordingly, the victim models will learn a latent connection between the unique pattern and the misclassification behavior (*i.e.*, backdoor). The backdoor trigger can serve as the secret key of ownership verification since it is stealthy for the adversary. The model owner can verify its ownership by triggering the misclassification (as shown in Figure 1).

However, backdoor-based methods have two fatal limitations, including harmfulness and ambiguity, as follows.

- 1) **Harmfulness:** Backdoor-based model watermarks incorporate patterns (*i.e.*, backdoor triggers) that can induce misclassification. Although they do not significantly compromise the model’s performance on the benign samples, the embedded pattern could pose a concealed threat that the adversary may exploit the backdoor to achieve specific malicious predictions [13], [27].
- 2) **Ambiguity:** The backdoor-based model watermarking methods fundamentally rely on misclassification. Consequently, the adversary can easily find some samples that are naturally misclassified by the model and verify its ownership independently, introducing ambiguity in ownership verification [11], [32].

We argue that the defects of the backdoor-based model watermarking methods described above can be attributed to the ‘zero-bit’ nature of the watermarking methods. The zero-bit backdoor watermark can only detect the presence or absence of the watermark but does not carry any information [50]. Backdoor-based methods directly embed the watermark into the predictions and only utilize the status (misclassified or not), for ownership verification. First, the pivotal status, ‘misclassified’, inevitably damages the model’s functionality, leading to harmfulness. Second, the zero-bit watermark can easily be forged because the misclassification of Deep Neural Network (DNN) is an inherently and commonly existing characteristic.

**Our Insight.** To tackle these problems, our insight is to explore an alternative space that can accommodate *multi-bit* watermark embedding without impacting model predictions. Drawing inspiration from eXplainable Artificial Intelligence (XAI) [39], we identify that the explanation generated by feature attribution methods offers a viable space for watermark embedding. Feature attribution, as an aspect of XAI, involves determining the importance of each feature in an input sample based on its relationship with the model’s prediction [46]. By leveraging this approach, it becomes feasible to embed multi-bit watermarks within the explanations of specific trigger samples without altering their corresponding predictions.

**Our Work.** In this paper, we propose ‘Explanation as a Watermark (EaaW)’, a harmless and multi-bit black-box model ownership verification method based on feature attribution. The fundamental framework of EaaW is illustrated in Figure 1. Specifically, by adding a constraint fitting the watermark to the loss function, we transform the explanation of a specific trigger sample into the watermark. We correspondingly design a watermark embedding and extraction algorithm inspired by a model-agnostic feature attribution algorithm, LIME [46]. Subsequently, the model owner can extract the watermark inside the model by inputting the trigger sample and employing the feature attribution algorithm.

Our contributions are summarized as follows:

- We revisit the existing backdoor-based model watermarking methods and reveal their fatal limitations. We point out that the intrinsic reason for those limitations is the ‘zero-bit’ nature of the backdoor-based watermarks.
- We propose a new black-box model watermarking paradigm named EaaW. EaaW embeds a multi-bit watermark into the explanation of a specific trigger sample while ensuring that the prediction remains correct.
- We propose a novel watermark embedding and extraction algorithm inspired by the feature attribution method in XAI. Our proposed watermark extraction method enables effective and efficient extraction of watermarks in the black-box scenario. It is also applicable for DNNs across a wide range of DL tasks, such as image classification and text generation.
- We conduct comprehensive experiments by applying EaaW to various models of both CV and NLP tasks. The experimental results demonstrate its effectiveness, distinctiveness, harmlessness, and resistance to various watermark-removal attacks and adaptive attacks.

The remaining parts of this paper are structured as follows: Section II provides an introduction to the background knowledge of DNN, Explainable Artificial Intelligence (XAI), and ownership verification of DNNs. Section III presents the problem formulation related to black-box DNN ownership verification. In Section IV, we propose a comprehensive insight, methodology, and implementation approach for EaaW. The effectiveness of EaaW is evaluated through experiments on image classification models and text generation models in Section V. Furthermore, additional experiments are conducted in Section VI to investigate the impact of EaaW on the watermarked models and analyze the security against ambiguity attacks. We conclude the paper in Section VII at the end.

## II. BACKGROUND

### A. Deep Neural Networks

Deep Neural Networks (DNN) have currently become the most popular AI models both in academia [2] and industry [42]. DNN models consist of multiple fundamental neurons, including linear projection, convolutions, and non-linear activation functions. These units are organized into layers within DNN models. Developers can employ DNN models to automatically acquire hierarchical data representations from the training data and use them to accomplish different tasks.

While training a DNN model  $\mathcal{M}$ , the model takes the raw training data  $\mathbf{x} \in \mathbb{R}^m$  as input, and then maps  $\mathbf{x}$  to the output prediction  $\mathbf{p} \in \mathbb{R}^n$  through a parametric function  $\mathbf{p} = f(\mathbf{x}; \Theta)$ . The parametric functions  $f(\cdot)$  are defined by both the architecture of the DNN model and the parameters  $\Theta$ . The developer then defines the loss function  $\mathcal{L}(\cdot)$  to measure the difference between the output prediction  $\mathbf{p}$  of the model and the true label  $\mathbf{y}$ . The objective of training the DNN model is equivalent to optimizing the parameters  $\Theta$  to have the minimum loss. The optimization problem can be formally defined as Eq. (1).

$$\Theta^* = \arg \min_{\Theta} \mathcal{L}(\mathbf{p}, \mathbf{y}) = \arg \min_{\Theta} \mathcal{L}(f(\mathbf{x}; \Theta), \mathbf{y}). \quad (1)$$

Recently, researchers have found that scaling the size of the models and datasets can make significant improvements in the models’ performance on various tasks, which leads to the rise of the large foundation models [42], [52]. Those large models often have more than 70 billion parameters and building such a large model requires a huge amount of training data, computational resources, and human expertise. Therefore, it is essential to protect the intellectual property rights of the model owners on the models.

### B. Explainable Artificial Intelligence

Due to the formidable capabilities of deep neural network (DNN) models, they have found extensive deployment across various domains. However, because of the intricate architectures of DNN, there is an urgent need to comprehend their internal mechanisms and gain insights into their outcomes [18]. In response to this demand for transparency, Explainable Artificial Intelligence (XAI) has been proposed as an approach to provide explanations for the black-box DNN models [9].

There are three main categories of XAI techniques based on the application stages, *i.e.*, pre-modeling explainability, explainable modeling, and post-modeling explainability [39]. In this paper, we mainly focus on a specific type of post-modeling explainability method, feature attribution, in XAI [46], [48]. Feature attribution is a method that helps users understand the importance of each feature in a model’s decision-making process. It calculates a real-value importance score for each feature based on its impact on the model’s output. The score could range from a positive value that shows its contribution to the prediction of the model, a zero that would mean that the feature has no contribution, to a negative value that means that removing that feature would increase the probability of the predicted class.

### C. Ownership Verification of DNN Models

Ownership verification of DNN models involves verifying whether the suspicious model is a copy of the model developed by another party (called the *victim model*) [50]. Watermark [1], [5], [30] and fingerprint [4], [22], [56] are two different solutions to implementing ownership verification, while the watermark is the most widely used ownership verification technique. Model watermark refers to embedding a unique signature (*i.e.*, watermark), which represents the identity of the model owner, into the model [1], [25], [53]. The model owner can extract the watermark from the model in case the model is illegally used by the adversary.

In general, model watermarking methods can be divided into two categories, white-box model watermarking methods and black-box model watermarking methods, as follows.

**White-box Model Watermarking Methods:** white-box model watermarking methods embed the watermark directly in the model parameters [35], [53], [54]. For instance, Uchida et al. propose to add a watermark regularization term into the loss function and embed the watermark through fine-tuning [53]. White-box model watermarking methods assume that the verifier can have full access to the suspicious model during verification. This assumption is difficult to realize in practical scenarios because the model is usually black-box in the real world. Such a limitation prevents the application of the

white-box watermarking methods. The watermark can also be embedded into the model via adjusting the architecture of the model [11], [35], or embedding external features [28], [29].

**Black-box Model Watermarking Methods:** Black-box model watermarking methods assume that the model owner can only observe the outputs from the suspicious model. Due to such a constraint, black-box methods are mainly based on the *backdoor attack* [13], [27]. Backdoor-based model watermarking methods utilize backdoor attacks to force a DNN model to remember specific patterns or features [1], [23]. The backdoor attack leads to misclassification when the DNN model encounters samples in a special dataset  $D_T$  called the trigger set. For ownership verification, the model owner can embed a non-transferable trigger set as watermarks into the protected model. The trigger set is unique to the watermarked model. The model owner keeps the trigger set secret and can thus verify ownership by triggering the misclassification. Backdoor-based methods are widely applicable to various tasks, such as image classification [1], [60], federated learning [51], [55], text generation [25], [31], and prompt [57], [58].

However, because the backdoor-based model watermarking methods embed a zero-bit watermark into the prediction of the models, they incur several disadvantages. First, although backdoor-based methods claim that they do not significantly compromise the functionality of the model with benign datasets, backdoor-based model ownership verification can still be harmful. Second, backdoor-based methods are based on misclassification and can only identify the presence or absence of a watermark. Adversaries can easily manipulate adversarial samples to verify their ownership on the victim model, leading to ambiguity in ownership verification [32]. To the best of our knowledge, BlackMarks [3] is the only multi-bit black-box watermarking method, based on the harmful backdoor attack. BlackMarks divides the output classes of the model into two groups. If the prediction class of the  $i$ -th trigger sample belongs to the first group, it means the  $i$ -th bit in the watermark is 0, otherwise 1. BlackMarks makes the sequential predictions of the trigger samples as a multi-bit watermark. However, the adversaries can create any bit string by rearranging the input trigger samples, leading to ambiguity.

Moreover, Maini et al. proposed a non-backdoor black-box model watermarking method called Dataset Inference (DI) [10], [36]. However, some recent studies demonstrated that DI may make misjudgments [29]. DI is also not able to embed a multi-bit watermark into the model. These limitations hinder its applicability in practice. How to design an effective and multi-bit black-box model watermarking method remains an important open question.

## III. PROBLEM FORMULATION

### A. Threat Model

In this section, we present the threat model regarding ownership verification of DNN models under the black-box setting. The model owner wants to train a DNN model and deploy it within its product. However, there exists the risk that an adversary may unlawfully copy or steal the model for personal gain. Such unauthorized behavior compromises the intellectual property rights of the model owner. Consequently, the model owner seeks an effective ownership verification

mechanism that is capable of confirming ownership over any third-party suspicious model through black-box access.

**Adversary’s Assumptions:** the adversary intends to acquire a high-performance DNN model by copying or stealing the victim model, which is developed by the other party. The adversary can attempt to remove the watermark inside the victim model without compromising its functionality. We assume that the adversary has the following capabilities:

- The adversary can conduct several watermark removal attack techniques trying to remove the watermark in the victim model, such as the fine-tuning attack, the model pruning attack, and the adaptive attack.
- The adversary has limited computational resources and data. The adversary does not have the capability of training a powerful model on its own.

**Defender’s Assumptions:** While protecting the copyright of DNN models, the defender is the actual developer and legal owner of the DNN models. The defender designs and trains the DNN model with its own efforts. The defender needs to implant a watermark into the model. Once the watermarked model is unauthorizedly used by other parties, the model owner can verify its ownership by extracting the watermark. In line with previous studies [1], [26], the capability of the defender is as follows:

- Before deploying the DNN model, the defender has full control of the training process, including the architecture of the model, the selection of the training dataset, and the implementation of the training techniques.
- After identifying potential infringement, the defender is unable to gain access to the architecture and parameters of the suspicious model. Instead, they can solely interact with the suspicious model through the API access, wherein they can input their data and get the output logits, *i.e.*, the prediction probabilities. We also investigate the scenario in which the defender can only get the predicted class (*i.e.*, label-only scenario) and the results can be found in Appendix D.

### B. Design Objectives

The objectives of designing a black-box model watermarking method can be summarized as follows:

- **Effectiveness:** Effectiveness signifies that the watermark needs to be properly embedded into the model. If the suspicious model actually originates from the victim model, the ownership verification algorithm can deterministically output a watermark which is similar to the victim’s pre-designed watermark.
- **Distinctiveness:** Distinctiveness represents that the watermark cannot be extracted from an independently trained model or with the independently selected secret key (*i.e.*, trigger samples). Distinctiveness guarantees that an independently trained model cannot be falsely claimed as others’ intellectual property.
- **Harmlessness:** Harmlessness refers to that the watermarked model should perform approximately as well as the primitive model without a watermark both on

the *benign dataset* and *trigger set*. It indicates that the ownership verification method has a negligible impact on the functionality of the model and does not implant any patterns that can trigger malicious predictions.

## IV. METHODOLOGY

In this section, we present the framework and methodology of our ‘Explanation as a Watermark (EaaW)’, a harmless and multi-bit black-box model ownership verification paradigm. Without loss of generality, we assume that the input data  $x \in \mathbb{R}^m$  and the model owner aims to embed a  $k$ -bit watermark  $\mathcal{W} \in \{-1, 1\}^k$ , *i.e.*, they are both 1-D vectors. The scenario where the input data space and the watermark are 2-D or 3-D can easily be transformed into the above scenario by flattening the high-dimension tensors into vectors. Note that here the watermark  $\mathcal{W}$  is not a bit string since its elements  $\mathcal{W}_i \in \{-1, 1\}$ . But the watermark can be transformed into a bit string by assigning 0 to elements of  $-1$ .

### A. Insight and Overview of EaaW

As discussed in Section II-C, backdoor-based model watermarks encounter two-fold drawbacks and challenges, namely harmfulness and ambiguity. These drawbacks arise primarily from the ‘zero-bit’ nature of the backdoor-based methods, where the watermark is embedded into the binary status of the model predictions. To tackle these challenges, a crucial question arises: ‘Can we find an alternative space to embed a multi-bit watermark without changing the predictions?’ Inspired by eXplainable Artificial Intelligence (XAI) and feature attribution, we propose EaaW. Our primary insight is that instead of directly watermarking the prediction classes of the model, the explanation generated by feature attribution algorithms can also serve as a suitable carrier for hiding information and embedding watermarks.

Figure 1 illustrates the framework of EaaW and provides a comparison with existing backdoor-based approaches. Unlike altering the prediction class of the trigger sample, EaaW leverages feature-attribution-based techniques to obtain the explanations for the trigger samples. The watermark hides within these output explanations.

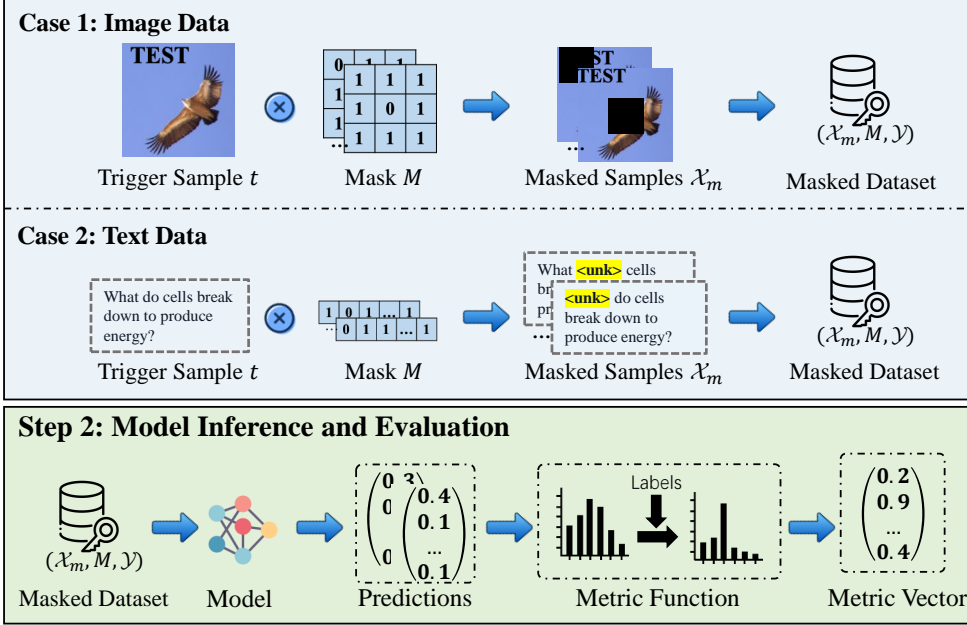
In general, our EaaW contains three stages, including (1) watermark embedding, (2) watermark extraction, and (3) ownership verification. The technical details of these stages are described in the following subsections.

### B. Watermark Embedding

As presented in Section III-B, the major objectives of an ownership verification mechanism are three-fold: effectiveness, distinctiveness, and harmlessness. In the watermark embedding stage, the model owner should embed the watermark by modifying the parameters  $\Theta$  of the trained model. Meanwhile, the model owner should preserve the functionality of the model after embedding the watermark. Therefore, we can define the watermark embedding task as a multi-task optimization problem based on the aforementioned objectives, which can be formalized as follows:

$$\begin{aligned} & \min_{\Theta} \mathcal{L}_1(f(\mathcal{X} \cup \mathcal{X}_T, \Theta), \mathcal{Y} \cup \mathcal{Y}_T) \\ & + r_1 \cdot \mathcal{L}_2(\text{explain}(\mathcal{X}_T, \mathcal{Y}_T, \Theta), \mathcal{W}), \end{aligned} \quad (2)$$

### Step 1: Local Sampling



### Step 3: Explanation Generation

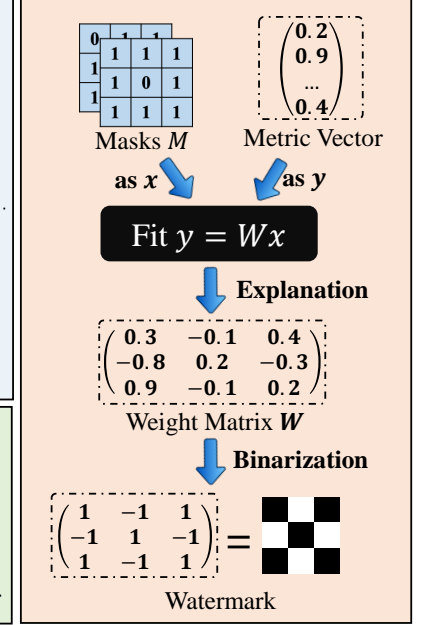


Fig. 2: The main pipeline of the watermark extraction algorithm based on feature attribution. First, we locally sample some masked samples by randomly masking a few basic parts of the trigger sample. Second, we input the masked dataset to get the prediction and calculate the metric vector. Finally, we fit a linear model to evaluate the importance of each basic part in the trigger sample. The sign of the explanation serves as the watermark.

where  $\Theta$  is the parameters of the model and  $\mathcal{W}$  is the target watermark.  $\mathcal{X}, \mathcal{Y}$  are the data and labels of the benign dataset, while  $\mathcal{X}_T, \mathcal{Y}_T$  are the data and labels of the trigger set. In our EaaW, we take the ground truth label of  $\mathcal{X}_T$  as  $\mathcal{Y}_T$  while backdoor-based methods exploit the targeted yet incorrect labels.  $\text{explain}(\cdot)$  is an XAI feature attribution algorithm used for watermark extraction in our EaaW, which will be introduced in Section IV-C.  $r_1$  is coefficient. There are two terms in Eq. (2). The first term  $\mathcal{L}_1(\cdot)$  represents the loss function of the model on the primitive task. It ensures that both the predictions on the benign dataset and trigger set remain unchanged, thereby preserving the model’s functionality. The second term  $\mathcal{L}_2(\cdot)$  quantifies the dissimilarity between the output explanation and target watermark. Optimizing  $\mathcal{L}_2(\cdot)$  can make the explanation similar to the watermark. We exploit the hinge-like loss as  $\mathcal{L}_2(\cdot)$  since it is proven to be beneficial for improving the resistance of the embedded watermark against watermark removal attacks [11]. We also explore using different watermark loss functions and conduct an ablation study in Appendix C. The hinge-like loss is shown as follows:

$$\mathcal{L}_2(\mathcal{E}, \mathcal{W}) = \sum_{i=1}^k \max(0, \varepsilon - \mathcal{E}_i \cdot \mathcal{W}_i), \quad (3)$$

where  $\mathcal{E} = \text{explain}(\mathcal{X}_T, \mathcal{Y}_T, \Theta)$ .  $\mathcal{E}_i$  and  $\mathcal{W}_i$  denote the  $i$ -th element of  $\mathcal{E}$  and  $\mathcal{W}$ , respectively.  $\varepsilon$  is the control parameter to encourage the absolute values of the elements in  $\mathcal{E}$  to be greater than  $\varepsilon$ . By optimizing Eq. (3), the watermark can be embedded into the sign of the explanation  $\mathcal{E}$ .

#### C. Watermark Extraction through Feature Attribution

The objective of model watermark embedding is to find the optimal model parameters  $\hat{\Theta}$  that makes Eq. (2) minimal.

In order to apply the popular gradient descent to optimize Eq. (2), we need to design a derivable and model-agnostic feature attribution explanation method. Inspired by a widely-used feature attribution algorithm, local interpretable model-agnostic explanation (LIME) [46], we design a LIME-based watermark extraction method to output the feature attribution explanation of the trigger sample.

The main insight of LIME is to locally sample some instances near the input data point and evaluate the importance of each feature via the output of these instances. We basically follow the insight of LIME and make some modifications to make the algorithm feasible for watermark embedding and extraction. The main pipeline of our watermark extraction algorithm is shown in Figure 2. In general, the designed watermark extraction based on LIME can be divided into three steps: (1) local sampling, (2) model inference and evaluation, and (3) explanation generation.

**Step 1: Local Sampling.** Assuming that the input  $x \in \mathbb{R}^m$ , local sampling is to generate several samples that are locally neighbor to the trigger sample  $x_T$ . First, we need to segment the input space into  $k$  basic parts, according to the length of the watermark  $\mathcal{W} \in \{-1, 1\}^k$ . The adjacent features can be combined as one basic part, and each basic part has  $\lfloor m/k \rfloor$  features. Redundant features are ignored since we aim to extract a watermark instead of explaining all the features.

The intuition of our algorithm is to evaluate which features are more influential to the prediction of a data point by systematically masking these basic parts. Thus, secondly, we randomly generate  $c$  masks  $M$ . Each mask in  $M$  is a binary vector (or matrix) with the same size as  $\mathcal{W}$ . We denote the  $i$ -th mask in  $M$  as  $M_i$ , and for each  $i$ ,  $M_i \in \{0, 1\}^k$ . Each

---

**Algorithm 1** Watermark Extraction Algorithm based on Feature Attribution.

---

**Input:** The trigger samples  $\mathcal{X}_T, \mathcal{Y}_T$ , the API access to the model  $f(\cdot; \Theta)$ .

**Output:** The watermark  $\tilde{\mathcal{W}}$  inside the model.

```

1:  $M = \text{random\_masks}(c, k)$ 
2:  $\mathcal{X}_m = M \otimes \mathcal{X}_T$ 
3:  $\mathbf{p} = f(\mathcal{X}_m; \Theta)$ 
4:  $\mathbf{v} = \mathcal{M}(\mathbf{p}, \mathcal{Y}_T)$ 
5:  $\mathbf{W} = (M^T M + \lambda I)^{-1} M^T \mathbf{v}$ 
6:  $\tilde{\mathcal{W}} = \text{zero\_like}(\mathbf{W})$ 
7: for  $i = 0$  to  $c - 1$  do
8:   if  $W_i \geq 0$  then
9:      $\tilde{\mathcal{W}}_i = 1$ 
10:  else
11:     $\tilde{\mathcal{W}}_i = -1$ 
12: return  $\tilde{\mathcal{W}}$ 

```

---

element in the mask corresponds to a basic part of the input.

After generating the masks, we construct the masked samples  $\mathcal{X}_m$  to constitute a dataset by masking the basic parts in the trigger sample according to the randomly generated masks. The masking operation can be denoted as  $\otimes$ .

$$\mathcal{X}_m = M \otimes \mathcal{X}_T. \quad (4)$$

Specifically, if the element in the mask  $M_i$  is 1, the corresponding basic part preserves the original value. Otherwise, the corresponding basic part should be replaced by a certain value if the element is 0. For example, for the image data, the pixels in the masked basic part could be aligned by 0. The tokens in the text data can be replaced by a special token ‘<unk>’ which represents an unknown token. The examples of the masked samples are shown in Figure 2.

**Step 2: Model Inference and Evaluation.** In this step, we input the masked dataset constructed in Step 1 into the model and get the predictions  $\mathbf{p} = f(\mathcal{X}_m; \Theta)$  of the masked samples. Note that in the label-only scenarios, the predictions  $\mathbf{p}$  are discretized as either 0 or 1, based on whether the sample is correctly classified. After that, we exploit a metric function  $\mathcal{M}(\cdot)$  to measure the quality of the predictions (compared with the ground-truth labels  $\mathcal{Y}_T$ ) and calculate the metric vector  $\mathbf{v} \in \mathbb{R}^c$  of the  $c$  masked samples via Eq. (5).

$$\mathbf{v} = \mathcal{M}(\mathbf{p}, \mathcal{Y}_T). \quad (5)$$

The metric function  $\mathcal{M}(\cdot)$  needs to be derivable and can provide a quantificational evaluation of the output. Users can customize it based on the specific DL task and prediction form. Since there usually exists a derivable metric function in DL tasks (*e.g.*, loss function), EaaW can easily be extended to various DL tasks such as image classification and text generation. The implementation details and results are shown in Section V-A and Section V-B, respectively.

**Step 3: Explanation Generation.** After calculating the metric

vector  $\mathbf{v}$ , the final step of the watermark extraction algorithm is to fit a linear model to evaluate the importance of each basic part and compute the importance scores. We take the metric vector  $\mathbf{v}$  as  $\mathbf{y}$  and the masks  $M$  as  $\mathbf{x}$ . In practice, we utilize ridge regression to improve the stability of the obtained weight matrix under different local samples. The weight matrix  $\mathbf{W}$  of the ridge regression represents the importance of each basic part. The weight matrix  $\mathbf{W}$  of the linear model can be calculated via the normal equation as shown in Eq. (6).

$$\mathbf{W} = (M^T M + \lambda I)^{-1} M^T \mathbf{v}. \quad (6)$$

In Eq. (6),  $\lambda$  is a hyper-parameter and  $I$  is a  $c \times c$  identity matrix. The watermark is embedded into the sign of the weight matrix’s elements. During watermark embedding, we utilize the weight matrix  $\mathbf{W}$  as  $\mathcal{E} = \text{explain}(\mathcal{X}_T, \mathcal{Y}_T, \Theta)$  to optimize the watermark embedding loss function Eq. (2). According to Eq. (6), the derivative of  $\mathbf{W}$  concerning  $\mathbf{v}$  exists, and the derivative of  $\mathbf{v}$  concerning the model parameters  $\Theta$  also exists in DNN, the whole watermark extraction algorithm is derivable due to the chain rule. Therefore, we can utilize the gradient descent algorithm to optimize Eq. (2) and embed the watermark into the model.

To further acquire the extracted watermark  $\tilde{\mathcal{W}} \in \{-1, 1\}^k$ , we binarize the weight matrix  $\mathbf{W}$  by applying the following binarization function  $\text{bin}(\cdot)$ .

$$\tilde{\mathcal{W}}_i = \text{bin}(W_i) = \begin{cases} 1, & W_i \geq 0 \\ -1, & W_i < 0 \end{cases}, \quad (7)$$

where  $\tilde{\mathcal{W}}_i, W_i$  is the  $i$ -th element of  $\tilde{\mathcal{W}}$  and  $\mathbf{W}$ . We show the pseudocode of the overall watermark extraction algorithm based on feature attribution in Algorithm 1.

#### D. Ownership Verification

In the event that the model owner finds a suspicious model deployed by an unauthorized party, the model owner can verify whether it is copied from the watermarked model by extracting the watermark from the suspicious model. Subsequently, the extracted watermark is compared with the model owner’s original watermark. The process is called the ownership verification process of DNN models.

Given a suspicious model  $\tilde{\Theta}$ , the model owner will first extract the watermark  $\tilde{\mathcal{W}}$  utilizing the trigger samples and the feature-attribution-based watermark extraction algorithm described in Section IV-C. We formalize the problem of comparing  $\tilde{\mathcal{W}}$  with  $\mathcal{W}$  as a hypothesis test, as follows.

**Proposition 1.** *Let  $\tilde{\mathcal{W}}$  be the watermark extracted from the suspicious model, and  $\mathcal{W}$  is the original watermark. Given the null hypothesis  $H_0$  :  $\tilde{\mathcal{W}}$  is independent of  $\mathcal{W}$  and the alternative hypothesis  $H_1$  :  $\tilde{\mathcal{W}}$  has an association or relationship with  $\mathcal{W}$ , the suspicious model can be claimed as an unauthorized copy if and only if  $H_0$  is rejected.*

In practice, we utilize Pearson’s chi-squared test [45] and calculate the p-value of the test. If the p-value is less than a significant level  $\alpha$ , the null hypothesis will be rejected and the suspicious model can be claimed as the intellectual property of the model owner. The pseudocode of the ownership verification algorithm is demonstrated in Algorithm 2.

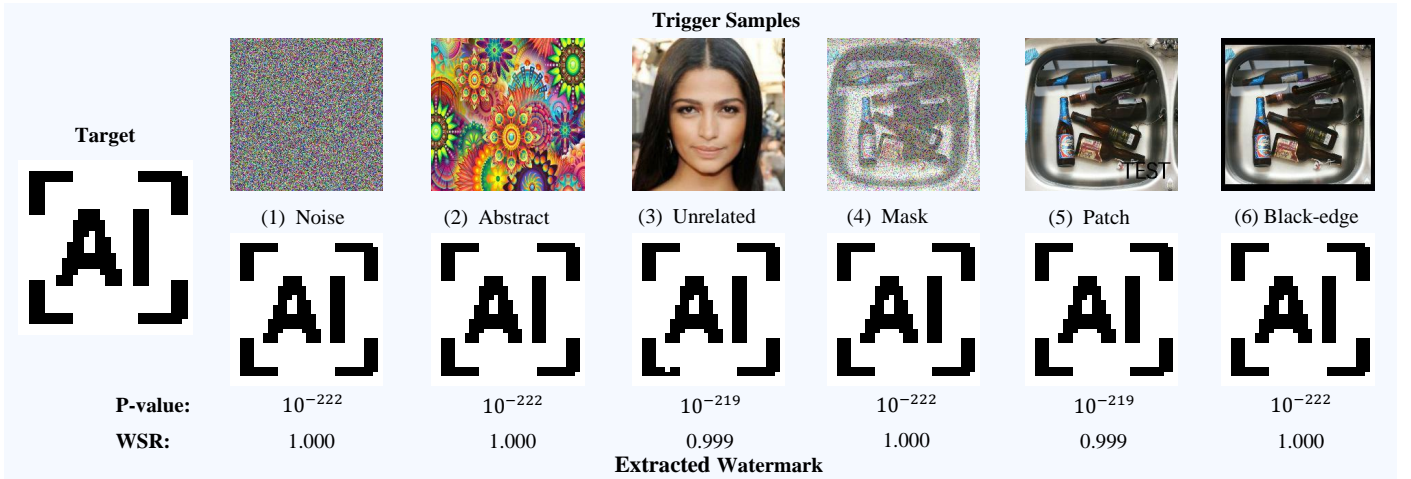


Fig. 3: The trigger samples (on the upper row) used to watermark image classification models and the corresponding extracted watermark (on the bottom row). The target watermark is shown on the left.

**Algorithm 2** Ownership verification algorithm based on hypothesis test.

**Input:** The trigger samples  $\mathcal{X}_T, \mathcal{Y}_T$ , the suspicious model  $\tilde{\Theta}$ , the original watermark  $\mathcal{W}$ , significant level  $\alpha$ .

**Output:** A boolean value indicating whether passing the ownership verification process.

- 1:  $\tilde{\mathcal{W}} = \text{explain}(\mathcal{X}_T, \mathcal{Y}_T, \tilde{\Theta})$
- 2:  $\tilde{\mathcal{W}} = \text{bin}(\tilde{\mathcal{W}})$
- 3:  $\text{p-value} = \chi^2 - \text{Test}(\tilde{\mathcal{W}}, \mathcal{W})$
- 4: **if**  $\text{p-value} \leq \alpha$  **then**
- 5:     **return** True
- 6: **else**
- 7:     **return** False

## V. EXPERIMENTS

In this section, we apply EaaW to two popular DL tasks: image classification and text generation. We evaluate the effectiveness, harmlessness, and distinctiveness of EaaW based on the objectives outlined in Section III-B. In addition, we also evaluate the resistance of EaaW against various watermark removal attacks [34]. We further provide an ablation study about some important hyper-parameters in EaaW. The comparison with backdoor-based watermarking methods is presented in Section VI-C. More experiments such as applying EaaW to the label-only scenario and the effects of the watermark losses can be found in the appendix.

**Watermark Metric.** In the hypothesis test, we set the significant level  $\alpha = 0.01$ , *i.e.*, if the p-value is less than 0.01, the null hypothesis will be rejected. In addition to evaluating the p-value of the hypothesis test, we also calculate the watermark success rate (WSR) between the extracted and original watermarks. The watermark success rate is the percentage of bits in the extracted watermark that match the original watermark. The WSR is formulated as follows.

$$\text{WSR} = \frac{1}{k} \sum_{i=1}^k \mathbb{I}\{\tilde{\mathcal{W}}_i = \mathcal{W}_i\}, \quad (8)$$

where  $k$  is the length of the watermark and  $\mathbb{I}\{\cdot\}$  is the indicator function. The lower the p-value and the greater the WSR, the closer the extracted watermark  $\tilde{\mathcal{W}}_i$  is to the original watermark  $\mathcal{W}_i$ , indicating a better effectiveness of watermark embedding.

### A. Results on Image Classification Models

1) *Experimental Settings:* In this section, we conduct the experiments on CIFAR-10 [24] and (a subset of) ImageNet [6] datasets with a popular convolutional neural network (CNN), ResNet-18 [17]. CIFAR-10 is a 10-class image classification dataset with  $32 \times 32$  color images. For the ImageNet dataset, we randomly select a subset containing 100 classes and there are 500 images per class for training and 100 images per class for testing. The images in the ImageNet dataset are resized to  $224 \times 224$ . We first pre-train the ResNet-18 models on CIFAR-10 and ImageNet datasets respectively for 300 epochs. The experiments with the ResNet-101 model can be found in Appendix C. Then we apply EaaW to embed the watermark into the models through a 30-epoch fine-tuning. Following the original LIME paper, we utilize the predicted probability of each sample’s target class to constitute the metric vector  $v$ .

To evaluate the effectiveness of EaaW, we implement 6 different trigger set construction methods from different backdoor watermarking methods, including (1) Noise [33]: utilizing Gaussian noise as trigger samples; (2) Abstract [1]: abstract images with no inherent meaning; (3) Unrelated [60]: images which are not related to the image classification tasks; (4) Mask [14]: images added with pseudo-random noise; (5) Patch [60]: adding some meaningful patch (*e.g.* ‘TEST’) into the images; (6) Black-edge: adding a black edge around the images. We take an image of ‘AI’ as the watermark embedded into the image classification models. We resize the ‘AI’ image into different sizes as watermarks with different bits. Examples of these trigger samples and the watermark image are shown in Figure 3.

2) *Evaluation on Effectiveness and Harmlessness:* Figure 3 and Table I present the experimental results of watermarking image classification models, demonstrating the successful embedding of the multi-bit watermark into these models via the utilization of EaaW. The p-values are far less than the

TABLE I: The testing accuracy (Test Acc.), the p-value of the hypothesis test, and watermark success rate (WSR) of embedding the watermark into image classification models via EaaW. ‘Length’ signifies the length of the embedded watermark.

Dataset	Length	Metric↓ Trigger→	No WM	Noise	Abstract	Unrelated	Mask	Patch	Black-edge
CIFAR-10	64	Test Acc.	90.54	90.49	90.53	90.49	90.46	90.38	90.37
		p-value	/	$10^{-13}$	$10^{-13}$	$10^{-13}$	$10^{-13}$	$10^{-13}$	$10^{-13}$
		WSR	/	1.000	1.000	1.000	1.000	1.000	1.000
	256	Test Acc.	90.54	90.53	90.54	90.28	90.49	90.11	90.35
		p-value	/	$10^{-54}$	$10^{-54}$	$10^{-54}$	$10^{-54}$	$10^{-54}$	$10^{-54}$
		WSR	/	1.000	1.000	1.000	1.000	1.000	1.000
	1024	Test Acc.	90.54	90.39	90.47	90.01	90.38	89.04	89.04
		p-value	/	$10^{-222}$	$10^{-222}$	$10^{-207}$	$10^{-222}$	$10^{-218}$	$10^{-222}$
		WSR	/	1.000	1.000	0.989	1.000	0.998	1.000
ImageNet	64	Test Acc.	76.38	75.80	76.04	76.00	75.98	75.76	75.78
		p-value	/	$10^{-13}$	$10^{-13}$	$10^{-13}$	$10^{-13}$	$10^{-13}$	$10^{-13}$
		WSR	/	1.000	1.000	1.000	1.000	1.000	1.000
	256	Test Acc.	76.38	75.86	75.96	76.36	76.06	76.06	75.60
		p-value	/	$10^{-54}$	$10^{-54}$	$10^{-54}$	$10^{-54}$	$10^{-54}$	$10^{-54}$
		WSR	/	1.000	1.000	1.000	1.000	1.000	1.000
	1024	Test Acc.	76.38	75.40	76.22	75.26	75.74	73.48	72.84
		p-value	/	$10^{-222}$	$10^{-222}$	$10^{-219}$	$10^{-222}$	$10^{-219}$	$10^{-222}$
		WSR	/	1.000	1.000	0.999	1.000	0.999	1.000

TABLE II: The p-value of the hypothesis test, and watermark success rate (WSR) with the watermarked model (Watermarked), independent model (Independent M.), and independent trigger (Independent T.) in the image classification task.

Dataset	Length	Trigger→ Scenario↓	Noise		Abstract		Unrelated		Mask		Patch		Black-edge	
			p-value	WSR	p-value	WSR	p-value	WSR	p-value	WSR	p-value	WSR	p-value	WSR
CIFAR-10	64	Watermarked	$10^{-13}$	1.000	$10^{-13}$	1.000	$10^{-13}$	1.000	$10^{-13}$	1.000	$10^{-13}$	1.000	$10^{-13}$	1.000
		Independent M.	0.115	0.656	0.811	0.500	0.265	0.625	0.550	0.422	0.740	0.531	0.651	0.547
		Independent T.	0.629	0.481	0.623	0.491	0.638	0.500	0.641	0.500	0.682	0.509	0.649	0.481
	256	Watermarked	$10^{-54}$	1.000	$10^{-54}$	1.000	$10^{-54}$	1.000	$10^{-54}$	1.000	$10^{-54}$	1.000	$10^{-54}$	1.000
		Independent M.	0.012	0.594	0.785	0.535	0.417	0.555	0.876	0.480	0.604	0.418	0.229	0.410
		Independent T.	0.323	0.483	0.273	0.487	0.340	0.485	0.273	0.487	0.409	0.488	0.349	0.473
	1024	Watermarked	$10^{-222}$	1.000	$10^{-222}$	1.000	$10^{-207}$	0.989	$10^{-222}$	1.000	$10^{-218}$	0.998	$10^{-222}$	1.000
		Independent M.	0.200	0.537	0.861	0.503	0.225	0.492	0.852	0.516	0.927	0.443	0.714	0.430
		Independent T.	0.521	0.457	0.721	0.463	0.618	0.448	0.452	0.459	0.544	0.459	0.450	0.450
ImageNet	64	Watermarked	$10^{-13}$	1.000	$10^{-13}$	1.000	$10^{-13}$	1.000	$10^{-13}$	1.000	$10^{-13}$	1.000	$10^{-13}$	1.000
		Independent M.	0.808	0.516	0.550	0.422	0.684	0.547	0.668	0.516	0.337	0.391	0.708	0.453
		Independent T.	0.761	0.491	0.761	0.491	0.749	0.491	0.755	0.494	0.757	0.500	0.751	0.494
	256	Watermarked	$10^{-54}$	1.000	$10^{-54}$	1.000	$10^{-54}$	1.000	$10^{-54}$	1.000	$10^{-54}$	1.000	$10^{-54}$	1.000
		Independent M.	0.943	0.484	0.806	0.441	0.737	0.527	0.693	0.434	0.198	0.574	0.646	0.523
		Independent T.	0.552	0.592	0.574	0.585	0.484	0.579	0.617	0.573	0.558	0.577	0.485	0.584
	1024	Watermarked	$10^{-222}$	1.000	$10^{-222}$	1.000	$10^{-219}$	0.999	$10^{-222}$	1.000	$10^{-219}$	0.999	$10^{-222}$	1.000
		Independent M.	0.910	0.483	0.874	0.525	0.916	0.480	0.482	0.486	0.219	0.500	0.181	0.433
		Independent T.	0.321	0.516	0.365	0.524	0.532	0.509	0.440	0.512	0.493	0.515	0.603	0.538

significant level  $\alpha$  and the WSRs are nearly equal to 1. Those results unequivocally establish the effectiveness of EaaW in facilitating watermark embedding.

In addition, based on the results in Table I, our watermarking method exhibits minimal impact on the model’s performance. Testing accuracy degrades less than 1% in most cases, indicating that the watermarked model maintains high functionality. Furthermore, it is observed that employing trigger samples close to the original images (such as ‘Patch’ and ‘Black-edge’) has a larger effect on the functionality of the model while achieving enhanced stealthiness. This implies a trade-off between harmlessness and stealthiness.

3) *Evaluation on Distinctiveness*: To evaluate the distinctiveness of EaaW, we also carry out experiments to test whether the watermark can be extracted with independently

trained models and independently selected trigger samples. The results are shown in Table II, indicating that the watermark extracted with independent models and independent triggers cannot pass the ownership verification process. The minimal p-value with independent models and independent triggers is 0.012 which is still  $> 0.01$  and far greater than the p-value of the watermarked model. The WSRs with independent models and triggers are mostly near 50%. Furthermore, the results also indicate that incorporating a higher number of bits in the watermark enhances distinctiveness and security. This is evidenced by the smaller p-values obtained when extracting a fewer-bit watermark using an independently trained model.

An example of the extracted watermarks with the watermarked model, independent model, and the independent trigger is shown in Figure 4. It shows that the extracted watermarks in the latter two scenarios are completely different from the



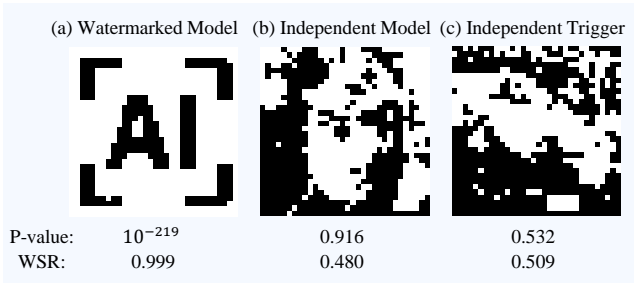


Fig. 4: An example of the extracted watermarks with the watermarked model, independent model, and independent trigger.

original watermark, further proving the distinctiveness.

## B. Results on Text Generation Models

1) *Experimental Settings:* In this section, we adopt EaaW to watermark the text generation models. The text generation model, especially the casual language model, is a type of language model that predicts the next token in a sequence of tokens [44]. Text generation models are widely used as the pre-trained foundation models in various natural language processing (NLP) tasks [42].

We take GPT-2 [44] as an example to evaluate EaaW on the text generation model since it is a representative open-sourced transformer-based model and many state-of-the-art large language models have similar structures. The experiments with another popular text generation model, *i.e.*, BERT [7], can be found in Appendix C. Four different datasets, including wikitext [38], bookcorpus [61], ptb-text-only [37], and lambada [43], are used to fine-tune the GPT-2 model and embed the multi-bit watermark. We randomly select a sequence in the training set as the trigger sample. We also randomly generate a  $k$ -bit string as the watermark and the examples of the text trigger samples and the embedded watermarks can be found in Appendix A. The lengths of the watermark are set to 32, 48, 64, 96, and 128. Additionally, different from the image classification model, we utilize the average prediction probabilities of the target tokens in the masked trigger sequence as the metric vector  $v$ . The implementation details can be found in Appendix A.

We utilize perplexity (PPL), which measures how well a language model can predict the next word in a sequence of words, as a metric to evaluate the harmlessness of EaaW on the text generation models. PPL is the exponential of the sequence cross-entropy. A lower PPL score indicates that the language model performs better at predicting the next word.

2) *Evaluation on Effectiveness and Harmlessness:* Table III shows the results of applying EaaW to the text generation models. In all the experiments, the watermarks are successfully embedded into the text generation models, with a significantly low p-value and 1.0 WSR. The results suggest the effectiveness of EaaW on the text generation models.

Table III also indicates that the functionality of the text generation models does not significantly drop after embedding the watermark, considering that PPL is an exponential metric. Also, the longer the length of the embedded watermark, the greater the impact on the model performance. However, a longer watermark can furnish more information for verification and better security.

TABLE III: The perplexity (PPL), the p-value of the hypothesis test, and watermark success rate (WSR) of embedding a watermark into text generation models via EaaW.

Dataset	Length→	No WM	32	48	64	96	128
wikitext	PPL	43.33	46.97	47.88	48.59	48.78	51.09
	p-value	/	$10^{-7}$	$10^{-10}$	$10^{-13}$	$10^{-20}$	$10^{-27}$
	WSR	/	1.000	1.000	1.000	1.000	1.000
bookcorpus	PPL	43.75	44.28	44.76	45.41	47.52	49.61
	p-value	/	$10^{-7}$	$10^{-10}$	$10^{-13}$	$10^{-20}$	$10^{-27}$
	WSR	/	1.000	1.000	1.000	1.000	1.000
ptb-text-only	PPL	39.49	40.98	42.41	42.68	45.52	48.99
	p-value	/	$10^{-7}$	$10^{-10}$	$10^{-13}$	$10^{-20}$	$10^{-27}$
	WSR	/	1.000	1.000	1.000	1.000	1.000
lambada	PPL	42.07	44.21	44.24	44.48	44.85	47.99
	p-value	/	$10^{-7}$	$10^{-10}$	$10^{-13}$	$10^{-20}$	$10^{-27}$
	WSR	/	1.000	1.000	1.000	1.000	1.000

3) *Evaluation on Distinctiveness:* Similar to the experiments conducted on the image classification models, we also test whether the watermark can be extracted from the independently trained language model or with independent trigger samples to validate the distinctiveness of EaaW.

From Table IV, we can find that the p-values with the independent model or independent trigger are greater than the significant level  $\alpha = 0.01$ , and the WSRs are around 0.5, which is similar to the results of the experiments on the image classification model. In addition, we can find that when the length of the watermark is relatively small, e.g. 32, the p-value with the independent model is small with a minimum 0.013 and close to the significant level. As the length of the watermark increases, the p-value with the independent model also increases, suggesting that embedding a watermark with more bits can obtain better security and distinctiveness.

## C. The Resistance to Watermark Removal Attacks

After obtaining the model from other parties, the adversaries may adopt various techniques to remove watermarks or circumvent detection. In this section, we explore whether our EaaW is resistant to them. Following the suggestions in [34], we consider three types of attacks, including fine-tuning attacks, model pruning attacks, and adaptive attacks.

1) *The Resistance to Fine-tuning Attack:* Fine-tuning refers to training the watermarked model with a local benign dataset for a few epochs. In the fine-tuning attack, the adversary may attempt to remove the watermark inside the model through fine-tuning. We fine-tune the EaaW-watermarked models with 20 epochs wheretraining has converged.

Figure 5 shows the log p-value and the WSR during the fine-tuning attack, while Figure 12 shows the extracted watermarks before and after the fine-tuning attack. As shown in Figure 5, the p-value and WSR fluctuate during fine-tuning, whereas the p-value is always significantly lower than the significant level  $\alpha$  (denoted by the purple dotted line) and the WSR is greater than 0.85. These results demonstrate the resistance of our EaaW to fine-tuning attacks. We argue that this is mostly because we did not change the label of watermarked samples during model training, leading to minor effects of fine-tuning compared to backdoor-based methods.

TABLE IV: The p-value of the hypothesis test, and watermark success rate (WSR) with the watermarked model (Watermarked), independent model (Independent M.), and independent trigger (Independent T.) in text generation modeling task.

Dataset	Length→	32		48		64		96		128	
	Scenario↓	p-value	WSR	p-value	WSR	p-value	WSR	p-value	WSR	p-value	WSR
wikitext	Watermarked	$10^{-7}$	1.000	$10^{-10}$	1.000	$10^{-13}$	1.000	$10^{-20}$	1.000	$10^{-27}$	1.000
	Independent M.	0.217	0.500	0.308	0.521	0.301	0.500	0.657	0.500	0.745	0.477
	Independent T.	0.457	0.450	0.424	0.413	0.414	0.422	0.484	0.435	0.693	0.466
bookcorpus	Watermarked	$10^{-7}$	1.000	$10^{-10}$	1.000	$10^{-13}$	1.000	$10^{-20}$	1.000	$10^{-27}$	1.000
	Independent M.	0.021	0.438	0.062	0.417	0.256	0.516	0.440	0.469	0.489	0.445
	Independent T.	0.296	0.394	0.565	0.492	0.355	0.419	0.725	0.506	0.520	0.475
ptb-text-only	Watermarked	$10^{-7}$	1.000	$10^{-10}$	1.000	$10^{-13}$	1.000	$10^{-20}$	1.000	$10^{-27}$	1.000
	Independent M.	0.040	0.406	0.152	0.438	0.070	0.469	0.333	0.521	0.594	0.445
	Independent T.	0.364	0.381	0.432	0.475	0.448	0.541	0.742	0.490	0.697	0.503
lambada	Watermarked	$10^{-7}$	1.000	$10^{-10}$	1.000	$10^{-13}$	1.000	$10^{-20}$	1.000	$10^{-27}$	1.000
	Independent M.	0.013	0.469	0.015	0.375	0.222	0.453	0.461	0.479	0.584	0.477
	Independent T.	0.284	0.481	0.351	0.408	0.254	0.394	0.634	0.500	0.602	0.531

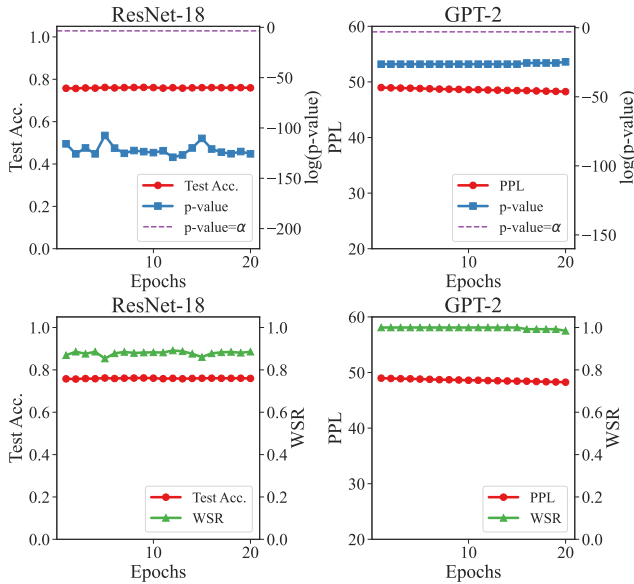


Fig. 5: Watermark success rate (WSR), the log p-value, and functionality evaluation (test accuracy or PPL) of watermarked ResNet-18 and GPT-2 against fine-tuning attack.

2) *The Resistance to Model-pruning Attack:* Model-pruning serves as a potential watermark-removal attack because it may prune watermark-related neurons. We exploit parameter pruning [16] as an example for discussion. Specifically, we prune the neurons in the model by zeroing out those with the lowest  $l_1$  norm. In particular, we use pruning rate to denote how many proportions of neuron are pruned.

As shown in Figure 6, the test accuracy of ResNet-18 drops while the PPL of GPT-2 increases, as the pruning rate increases. It indicates the degradation of the functionality of the model. However, the p-value of the pruned model negligibly changes and is lower than the significant level  $\alpha$ . Besides, the WSR is still greater than 0.9. These results suggest that our EaaW resists to model-pruning attack.

3) *The Resistance to Adaptive Attacks:* In practice, the adversaries may know the existence of our EaaW and design

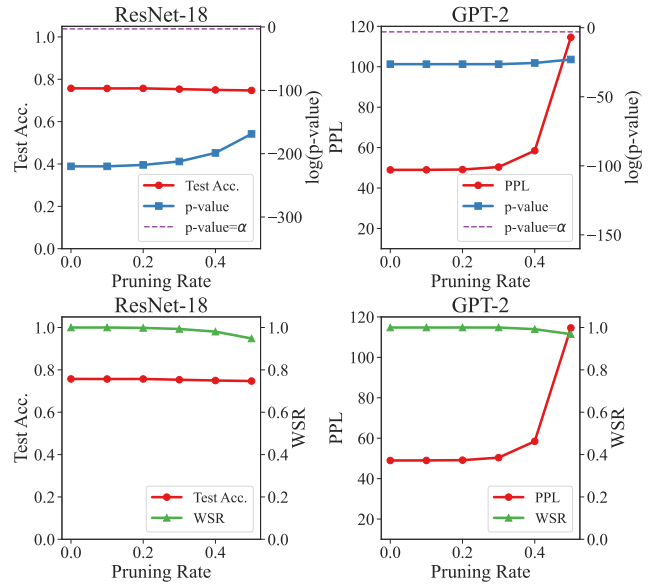


Fig. 6: Watermark success rate (WSR), the log p-value, and functionality evaluation (test accuracy or PPL) of watermarked ResNet-18 and GPT-2 against model-pruning attack.

adaptive attacks to circumvent it. Specifically, they may try to remove the watermark or interfere with the watermark extraction by manipulating the explanation of the input data. Existing techniques for manipulating explanations can be classified into two categories: (1) modifying model parameters [19], [41] or (2) modifying the inputs (*i.e.*, the adversarial attack against XAI) [12]. In this section, we hereby present the results under the first type of attacks in two representative scenarios, namely the *overwriting attack* and the *unlearning attack*. The discussion about the second one can be found in Appendix E.

*Scenario 1 (Overwriting Attack):* In this scenario, we assume that the adversary knows the procedure of the EaaW method, but has no knowledge of the trigger samples and the target watermark used by the model owner. Therefore, the adversary can independently generate the trigger samples and the watermark, and then embed them into the model,

TABLE V: Watermark success rate (WSR), the log p-value, and functionality evaluation (test accuracy or PPL) of ResNet-18 and GPT-2 against overwriting attack and unlearning attack.

Model	Metric ↓	Before	After Overwriting	After Unlearning
ResNet-18	Test Acc.	75.72	69.18	73.62
	p-value	$10^{-222}$	$10^{-134}$	$10^{-127}$
	WSR	1.000	0.899	0.888
GPT-2	PPL	48.99	50.29	48.96
	p-value	$10^{-27}$	$10^{-18}$	$10^{-24}$
	WSR	1.000	0.906	0.969

attempting to overwrite the watermark embedded before. This category of adaptive attack is called the *overwriting attack*.

The experimental results of the overwriting attack are shown in Table V. We conduct a 10-epoch fine-tuning to simulate the overwriting process and the models have already converged after 10 epochs. After the overwriting attack, the functionality of both the watermarked ResNet-18 and the watermarked GPT-2 decreases, while the p-values are still low and the WSRs are close to 0.9. It indicates that the overwriting attack cannot effectively remove our EaaW watermark.

*Scenario 2 (Unlearning Attack):* In this scenario, we assume that the adversary knows the embedded watermark, but still has no knowledge of the trigger samples. As such, the adversary will randomly select some trigger samples and try to unlearn the watermark by updating the model in the direction opposite to the watermarking gradient. We make this assumption because the target watermark can often be conjectured. For example, the watermark may be the logo of the corporation or the profile photo of the individual developer. This type of attack is called the *unlearning attack*. The adversary uses the following loss function to unlearn the watermark:

$$\min_{\hat{\Theta}} \mathcal{L}_1(f(\mathcal{X}, \hat{\Theta}), \mathcal{Y}) - r_1 \mathcal{L}_2(\text{explain}(\tilde{\mathcal{X}}_T, \tilde{\mathcal{Y}}_T, \hat{\Theta}), \mathcal{W}). \quad (9)$$

The experimental results of the unlearning attack are illustrated in Table V. The results demonstrate that our EaaW also resists to unlearning attack. Specifically, the WSRs drop only 0.112 and 0.031, respectively. The watermark can still be extracted from the model and the ownership can still be verified with low p-values.

#### D. Ablation Study

In this section, we conduct the ablation study to investigate the effect of some important hyper-parameters used in EaaW, such as the size of the trigger samples, the number  $c$  of the masks, and the coefficient  $r_1$ . More ablation studies can be found in Appendix C.

1) *Effect of the Size of the Trigger Samples:* In EaaW, the trigger sample  $\mathcal{X}_T$  and its label  $\mathcal{Y}_T$  can be considered as the secret key to extracting the watermark. Holding one secret key is enough for most cases, while multiple secret keys can further enhance the security of EaaW. In this section, we select 1, 2, 5, 10, and 20 trigger samples and test the effectiveness of EaaW with different numbers of trigger samples. The results are illustrated in Figure 7. As the size of the trigger samples increases, the functionality of the watermarked model and the WSR degrades, and the p-value increases. But generally

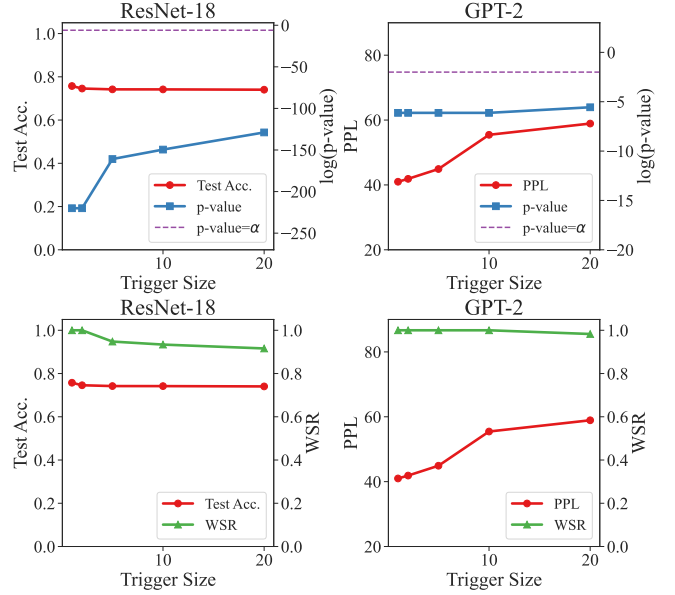


Fig. 7: The Watermark success rate (WSR), the log p-value, and the functionality evaluation metrics (test accuracy or PPL) of watermarked ResNet-18 and GPT-2 with different sizes of the trigger samples.

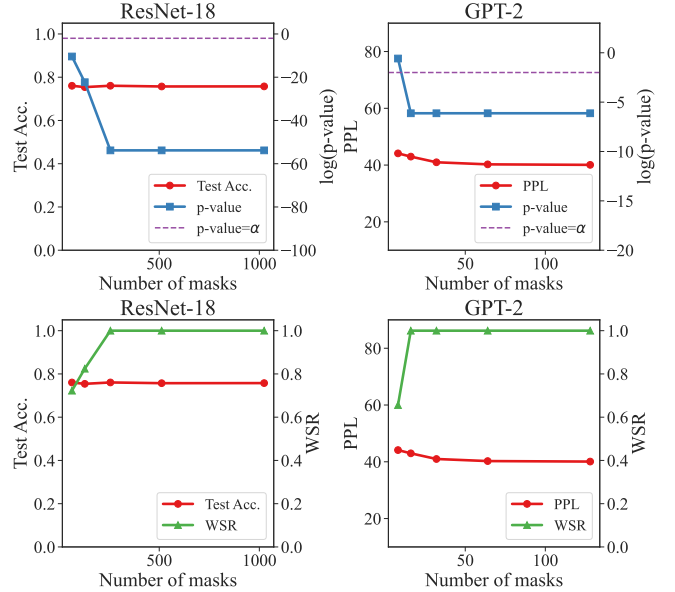


Fig. 8: The watermark success rate (WSR), the log p-value, and the functionality evaluation metrics (test accuracy or PPL) of ResNet-18 and GPT-2 with different numbers of masks.

speaking, the model is capable of accommodating multiple trigger samples and the model owner can choose the size of trigger samples based on its practical requirements.

2) *Effect of the Number of the Masks:* In this section, we study the effect of the number  $c$  of the masks and masked samples. We set  $c$  to be 64 to 1024 to embed a 256-bit watermark into ResNet-18 and set  $c$  to be 8 to 128 to embed a 32-bit watermark into GPT-2. The results are in Figure 8. The results indicate that using a low  $c$  may lead to the failure of embedding the watermark. A small number of masked

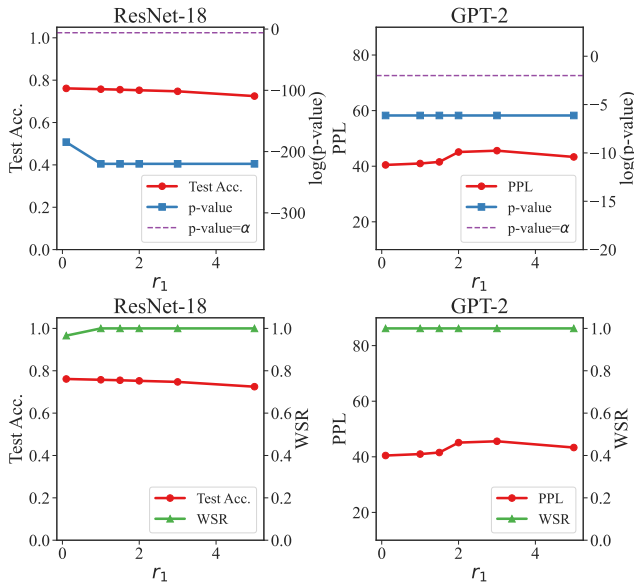


Fig. 9: The watermark success rate (WSR), the log p-value, and the functionality evaluation (test accuracy or PPL) of watermarked ResNet-18 and GPT-2 with different  $r_1$ .

samples can not effectively evaluate the importance of each basic part, and thus the feature attribution algorithm does not work well in that case. On the contrary, sampling more masked samples contributes to the extraction of the watermark and can better preserve the functionality of the watermarked model. However, the overhead of embedding and extracting the watermark also increases. There is a trade-off between functionality and efficiency.

3) *Effect of Coefficient  $r_1$* :  $r_1$  is the coefficient of the watermark loss in Eq. (2).  $r_1$  governs the balance between embedding the watermark and preserving model functionality. To assess its impact, we varied  $r_1$  across values of 0.1, 1.0, 1.5, 2.0, 3.0, and 5.0 for evaluation purposes. Figure 9 reveals that employing a larger  $r_1$  can potentially exert a more pronounced negative effect on the functionality of the watermarked model; conversely, adopting a smaller  $r_1$  may not entirely ensure complete watermark embedding within the model’s framework. Nevertheless, in most scenarios, successful watermark integration into the model was achieved overall.

## VI. DISCUSSION AND ANALYSIS

### A. How EaaW Affect the Watermarked Model?

In this section, we explore how EaaW affects the watermarked model. Inspired by [20], we analyze the effect of EaaW by visualizing the intermediate features of both the benign samples and the trigger sample. We first randomly select 100 images per class from the training dataset. Subsequently, we input those data into the model and get the output of the features by the penultimate layer. To further analyze these features, we employ the kernel principal component analysis (Kernel PCA) algorithm for dimensionality reduction, reducing those features to 2 dimensions. The visualization of these reduced features is presented in Figure 10. Notably, the feature corresponding to the trigger sample is denoted as a star.

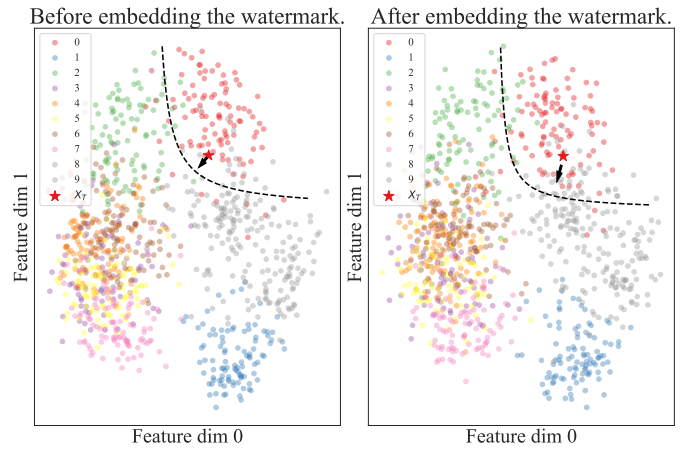


Fig. 10: The visualization of the feature representations of the training data before and after embedding the watermark. Those of the trigger sample is marked as ‘star’ and the trigger sample belongs to the class 0 colored by red. The feature representations of all the samples do not significantly change. Instead, the direction of the trigger sample to the decision boundary is transformed. (Better viewed in color)

From Figure 10, we can see that the intermediate feature representations are generally unaffected before and after embedding the watermark using EaaW. The feature of the trigger sample continues to reside within the cluster corresponding to its respective class (the red class numbered 0), thereby demonstrating the harmlessness of EaaW. Additionally, as depicted in Figure 10, EaaW actually changes the direction of the trigger sample to the decision boundary of the model, that is, the direction of the trigger sample’s gradient. By embedding a multi-bit watermark into the sign of this gradient, EaaW achieves successful model watermarking without altering the prediction of the trigger sample.

### B. Security Analysis against Ambiguity Attack

When the adversary acquires the watermarked model, the adversary can attempt to forge a fake watermark to establish its ownership of the watermarked model. If both the true model owner and the adversary can independently authenticate their copyright claims, it becomes impossible to ascertain the actual ownership. This type of attack is named *ambiguity attack* [11] (or false claim attack [32]). The definition of the ambiguity attack for our EaaW is as follows.

**Definition 1** (Ambiguity Attack). *Given a watermarked model  $\hat{\Theta}$ , the objective of the ambiguity attack is to forge a fake trigger sample  $\tilde{X}_T, \tilde{Y}_T$  that can be utilized to extract its own watermark  $\hat{W}$  and pass the ownership verification algorithm described in Algorithm 2.*

As our approach involves embedding a multi-bit watermark into the model, the EaaW technique offers superior security compared to the zero-bit backdoor-based model watermarking methods. Intuitively, assuming that the probability of a successful ambiguity attack against a one-bit (or zero-bit) watermark method is  $1/\xi$ , then the probability of a successful ambiguity attack against a  $k$ -bit watermark method is  $1/\xi^k$ . As such, for a not-too-small length  $k$  of the watermark, our proposed

TABLE VI: The watermark success rate (WSR), the harmless degree  $H$  (larger is better), and test accuracy (Test Acc.) using the backdoor-based model watermarking method and EaaW in the image classification task.

Dataset	Length / Trigger Size	Trigger→ Method↓	Noise [33]			Unrelated [60]			Mask [14]			Patch [60]			Black-edge		
			Test Acc.	$H$	WSR	Test Acc.	$H$	WSR	Test Acc.	$H$	WSR	Test Acc.	$H$	WSR	Test Acc.	$H$	WSR
CIFAR-10	64	No WM	90.54	/	/	90.54	/	/	90.54	/	/	90.54	/	/	90.54	/	/
		Backdoor	90.38	89.74	<b>1.000</b>	88.74	88.10	<b>1.000</b>	90.34	89.71	0.984	84.28	83.64	<b>1.000</b>	86.24	85.60	<b>1.000</b>
		EaaW	<b>90.49</b>	<b>90.48</b>	<b>1.000</b>	<b>90.49</b>	<b>90.48</b>	<b>1.000</b>	<b>90.46</b>	<b>90.47</b>	<b>1.000</b>	<b>90.38</b>	<b>90.39</b>	<b>1.000</b>	<b>90.37</b>	<b>90.38</b>	<b>1.000</b>
	256	No WM	90.54	/	/	90.54	/	/	90.54	/	/	90.54	/	/	90.54	/	/
		Backdoor	90.33	87.77	<b>1.000</b>	87.99	85.43	<b>1.000</b>	90.28	87.72	<b>1.000</b>	<b>90.11</b>	87.75	<b>1.000</b>	90.07	87.51	<b>1.000</b>
		EaaW	<b>90.53</b>	<b>90.52</b>	<b>1.000</b>	<b>90.28</b>	<b>90.27</b>	<b>1.000</b>	<b>90.49</b>	<b>90.50</b>	<b>1.000</b>	<b>90.11</b>	<b>90.12</b>	<b>1.000</b>	<b>90.35</b>	<b>90.36</b>	<b>1.000</b>
	1024	No WM	90.54	/	/	90.54	/	/	90.54	/	/	90.54	/	/	90.54	/	/
		Backdoor	90.19	80.19	0.977	88.14	77.93	0.997	90.17	79.93	<b>1.000</b>	<b>90.03</b>	79.79	<b>1.000</b>	<b>89.81</b>	79.57	<b>1.000</b>
		EaaW	<b>90.39</b>	<b>90.38</b>	<b>1.000</b>	<b>90.01</b>	<b>90.00</b>	0.989	<b>90.38</b>	<b>90.39</b>	<b>1.000</b>	89.04	<b>89.05</b>	0.998	89.04	<b>89.05</b>	<b>1.000</b>
ImageNet	64	No WM	76.38	/	/	76.38	/	/	76.38	/	/	76.38	/	/	76.38	/	/
		Backdoor	73.16	72.67	0.766	75.94	75.30	<b>1.000</b>	75.06	74.42	<b>1.000</b>	74.18	73.54	<b>1.000</b>	73.96	73.32	<b>1.000</b>
		EaaW	<b>75.80</b>	<b>75.79</b>	<b>1.000</b>	<b>76.00</b>	<b>75.99</b>	<b>1.000</b>	<b>75.98</b>	<b>75.99</b>	<b>1.000</b>	<b>75.76</b>	<b>75.77</b>	<b>1.000</b>	<b>75.78</b>	<b>75.79</b>	<b>1.000</b>
	256	No WM	76.38	/	/	76.38	/	/	76.38	/	/	76.38	/	/	76.38	/	/
		Backdoor	73.70	71.14	<b>1.000</b>	75.92	73.36	<b>1.000</b>	74.08	71.52	<b>1.000</b>	70.34	67.80	0.992	71.10	68.59	0.980
		EaaW	<b>75.86</b>	<b>75.85</b>	<b>1.000</b>	<b>76.36</b>	<b>76.35</b>	<b>1.000</b>	<b>76.06</b>	<b>76.07</b>	<b>1.000</b>	<b>76.06</b>	<b>76.07</b>	<b>1.000</b>	<b>75.60</b>	<b>75.61</b>	<b>1.000</b>
	1024	No WM	76.38	/	/	76.38	/	/	76.38	/	/	76.38	/	/	76.38	/	/
		Backdoor	73.56	64.22	0.912	<b>75.86</b>	65.62	<b>1.000</b>	74.86	64.62	<b>1.000</b>	73.92	63.68	<b>1.000</b>	<b>74.32</b>	64.08	<b>1.000</b>
		EaaW	<b>75.40</b>	<b>75.39</b>	<b>1.000</b>	75.26	<b>75.25</b>	0.999	<b>75.74</b>	<b>75.75</b>	<b>1.000</b>	<b>73.48</b>	<b>73.49</b>	0.999	72.84	<b>72.85</b>	<b>1.000</b>

EaaW can withstand ambiguity attacks. To support this claim, we present the following proposition.

**Proposition 2.** *Given the length of the watermark  $k$ , the probability of a successful ambiguity attack is  $1/2^k$ .*

*Proof:* Assuming that the adversary has no knowledge of the trigger sample used for ownership verification. When the adversary tries to forge a trigger sample by random selection, the probability of each bit being the correct bit can be assumed as  $1/2$ . Since the explanation output by the feature attribution algorithm depends on all the features of the input data, the probability of the explanation correctly matching the watermark is  $1/2^k$ . ■

Proposition 2 shows that the time complexity of the ambiguity attack against EaaW is exponential concerning the length  $k$  of the watermark, indicating that our watermarking method is hard to forge by the adversary and is resistant to ambiguity attack. Furthermore, Proposition 2 also suggests utilizing a multi-bit watermark can obtain better security.

### C. The Comparison to Backdoor Watermarks

Backdoor-based model watermarks are currently the most representative and popular black-box model ownership verification techniques. Arguably, the primary differences among these various backdoor-based approaches lie in their distinct construction of the trigger set [50]. Recall that existing literature has already shed light on the ambiguous nature of backdoor-based watermarks [21], [32], while our Section VI-B demonstrates that our EaaW technique remains resilient against ambiguity attacks. Accordingly, this section primarily focuses on the comparison between various backdoor-based methods [14], [33], [60] and our EaaW in terms of effectiveness and harmless degree. Inspired by the definition in [15], we define the *harmless degree*  $H$  as the metric for evaluating the level of harmless degree.  $H$  is defined as the accuracy achieved both on the benign testing dataset  $\mathcal{X}$ ,  $\mathcal{Y}$  and the trigger set  $\mathcal{X}_T$ ,  $\mathcal{Y}_T$

with the ground-truth labels, as follows.

$$H = \frac{1}{|\mathcal{X} \cup \mathcal{X}_T|} \sum_{\mathbf{x} \in \mathcal{X} \cup \mathcal{X}_T} \mathbb{I}\{f(\mathbf{x}; \Theta) = g(\mathbf{x})\}, \quad (10)$$

where  $\mathbb{I}\{\cdot\}$  is the indicator function and  $g(\mathbf{x})$  always output the ground-truth label of  $\mathbf{x}$ . A larger  $H$  means the watermarks have less effect on the utility of the models.

As shown in Table VI, the watermarking effectiveness of our EaaW is on par with or even better than that of the baseline backdoor-based methods. Regarding harmless degree, our EaaW approach outperforms the backdoor-based techniques as evidenced by higher harmless degrees  $H$ . For example, the harmless degree  $H$  of our EaaW is nearly 10% higher than that of backdoor-based watermarks in all cases with trigger size 1024. Note that backdoor-based watermarks introduce backdoors that can be exploited by adversaries to generate specific malicious predictions, although they do not compromise performance on benign samples.

## VII. CONCLUSION

In this paper, we revealed that the widely applied backdoor-based model watermarking methods have two major drawbacks, including harmless degree and ambiguity. We found out that those limitations can both be attributed to that the backdoor-based watermark utilizes misclassification to embed a ‘zero-bit’ watermark into the model. To tackle these issues, we proposed a harmless and multi-bit model ownership verification method, named Explanation as a Watermark (EaaW), inspired by XAI. EaaW is the first to introduce the insight of embedding the multi-bit watermark into the explanation output by feature attribution methods. We correspondingly designed a feature attribution-based watermark embedding and extraction algorithm. Our empirical experiments demonstrated the effectiveness, distinctiveness, and harmless degree of EaaW. We hope our EaaW can provide a new angle and deeper understanding of model ownership verification to facilitate secure and trustworthy model deployment and sharing.

## REFERENCES

- [1] Y. Adi, C. Baum, M. Cisse, B. Pinkas, and J. Keshet, "Turning your weakness into a strength: Watermarking deep neural networks by backdooring," in *USENIX Security Symposium*, 2018, pp. 1615–1631.
- [2] T. Brown, B. Mann, N. Ryder, M. Subbiah, J. D. Kaplan, P. Dhariwal, A. Neelakantan, P. Shyam, G. Sastry, A. Askell *et al.*, "Language models are few-shot learners," *Advances in Neural Information Processing Systems*, vol. 33, pp. 1877–1901, 2020.
- [3] H. Chen, B. D. Rouhani, and F. Koushanfar, "Blackmarks: Black-box multibit watermarking for deep neural networks," *arXiv preprint arXiv:1904.00344*, 2019.
- [4] J. Chen, J. Wang, T. Peng, Y. Sun, P. Cheng, S. Ji, X. Ma, B. Li, and D. Song, "Copy, right? a testing framework for copyright protection of deep learning models," in *IEEE Symposium on Security and Privacy*, 2022, pp. 824–841.
- [5] T. Cong, X. He, and Y. Zhang, "Sslguard: A watermarking scheme for self-supervised learning pre-trained encoders," in *ACM SIGSAC Conference on Computer and Communications Security*, 2022, pp. 579–593.
- [6] J. Deng, W. Dong, R. Socher, L.-J. Li, K. Li, and L. Fei-Fei, "Imagenet: A large-scale hierarchical image database," in *IEEE Conference on Computer Vision and Pattern Recognition*, 2009, pp. 248–255.
- [7] J. Devlin, M.-W. Chang, K. Lee, and K. Toutanova, "Bert: Pre-training of deep bidirectional transformers for language understanding," *arXiv preprint arXiv:1810.04805*, 2018.
- [8] A. Dosovitskiy, L. Beyer, A. Kolesnikov, D. Weissenborn, X. Zhai, T. Unterthiner, M. Dehghani, M. Minderer, G. Heigold, S. Gelly *et al.*, "An image is worth 16x16 words: Transformers for image recognition at scale," in *International Conference on Learning Representations*, 2020.
- [9] R. Dwivedi, D. Dave, H. Naik, S. Singhal, R. Omer, P. Patel, B. Qian, Z. Wen, T. Shah, G. Morgan *et al.*, "Explainable ai (xai): Core ideas, techniques, and solutions," *ACM Computing Surveys*, vol. 55, no. 9, pp. 1–33, 2023.
- [10] A. Dziedzic, H. Duan, M. A. Kaleem, N. Dhawan, J. Guan, Y. Cattan, F. Boenisch, and N. Papernot, "Dataset inference for self-supervised models," *Advances in Neural Information Processing Systems*, vol. 35, pp. 12 058–12 070, 2022.
- [11] L. Fan, K. W. Ng, and C. S. Chan, "Rethinking deep neural network ownership verification: Embedding passports to defeat ambiguity attacks," *Advances in Neural Information Processing Systems*, vol. 32, 2019.
- [12] A. Ghorbani, A. Abid, and J. Zou, "Interpretation of neural networks is fragile," in *AAAI conference on artificial intelligence*, vol. 33, no. 01, 2019, pp. 3681–3688.
- [13] T. Gu, K. Liu, B. Dolan-Gavitt, and S. Garg, "Badnets: Evaluating backdooring attacks on deep neural networks," *IEEE Access*, vol. 7, pp. 47 230–47 244, 2019.
- [14] J. Guo and M. Potkonjak, "Watermarking deep neural networks for embedded systems," in *IEEE/ACM International Conference on Computer-Aided Design*, 2018, pp. 1–8.
- [15] J. Guo, Y. Li, L. Wang, S.-T. Xia, H. Huang, C. Liu, and B. Li, "Domain watermark: Effective and harmless dataset copyright protection is closed at hand," in *Advances in Neural Information Processing Systems*, 2023.
- [16] S. Han, J. Pool, J. Tran, and W. Dally, "Learning both weights and connections for efficient neural network," *Advances in Neural Information Processing Systems*, vol. 28, 2015.
- [17] K. He, X. Zhang, S. Ren, and J. Sun, "Deep residual learning for image recognition," in *IEEE Conference on Computer Vision and Pattern Recognition*, 2016, pp. 770–778.
- [18] Y. He, J. Lou, Z. Qin, and K. Ren, "Finer: Enhancing state-of-the-art classifiers with feature attribution to facilitate security analysis," in *ACM SIGSAC Conference on Computer and Communications Security*, 2023, pp. 416–430.
- [19] J. Heo, S. Joo, and T. Moon, "Fooling neural network interpretations via adversarial model manipulation," *Advances in Neural Information Processing Systems*, vol. 32, 2019.
- [20] G. Hua and A. B. J. Teoh, "Deep fidelity in dnn watermarking: A study of backdoor watermarking for classification models," *Pattern Recognition*, vol. 144, 2023.
- [21] G. Hua, A. B. J. Teoh, Y. Xiang, and H. Jiang, "Unambiguous and high-fidelity backdoor watermarking for deep neural networks," *IEEE Transactions on Neural Networks and Learning Systems*, 2023.
- [22] H. Jia, H. Chen, J. Guan, A. S. Shamsabadi, and N. Papernot, "A zest of lime: Towards architecture-independent model distances," in *International Conference on Learning Representations*, 2021.
- [23] H. Jia, C. A. Choquette-Choo, V. Chandrasekaran, and N. Papernot, "Entangled watermarks as a defense against model extraction," in *USENIX Security Symposium*, 2021, pp. 1937–1954.
- [24] A. Krizhevsky, G. Hinton *et al.*, "Learning multiple layers of features from tiny images," *Master's thesis, University of Tront*, 2009.
- [25] P. Li, P. Cheng, F. Li, W. Du, H. Zhao, and G. Liu, "Plmmark: A secure and robust black-box watermarking framework for pre-trained language models," in *AAAI Conference on Artificial Intelligence*, vol. 37, no. 12, 2023, pp. 14 991–14 999.
- [26] Y. Li, Y. Bai, Y. Jiang, Y. Yang, S.-T. Xia, and B. Li, "Untargeted backdoor watermark: Towards harmless and stealthy dataset copyright protection," *Advances in Neural Information Processing Systems*, vol. 35, pp. 13 238–13 250, 2022.
- [27] Y. Li, Y. Jiang, Z. Li, and S.-T. Xia, "Backdoor learning: A survey," *IEEE Transactions on Neural Networks and Learning Systems*, 2022.
- [28] Y. Li, L. Zhu, X. Jia, Y. Bai, Y. Jiang, S.-T. Xia, and X. Cao, "Move: Effective and harmless ownership verification via embedded external features," *arXiv preprint arXiv:2208.02820*, 2022.
- [29] Y. Li, L. Zhu, X. Jia, Y. Jiang, S.-T. Xia, and X. Cao, "Defending against model stealing via verifying embedded external features," in *AAAI Conference on Artificial Intelligence*, vol. 36, no. 2, 2022, pp. 1464–1472.
- [30] Z. Li, C. Wang, S. Wang, and C. Gao, "Protecting intellectual property of large language model-based code generation apis via watermarks," in *ACM SIGSAC Conference on Computer and Communications Security*, 2023, pp. 2336–2350.
- [31] J. H. Lim, C. S. Chan, K. W. Ng, L. Fan, and Q. Yang, "Protect, show, attend and tell: Empowering image captioning models with ownership protection," *Pattern Recognition*, vol. 122, 2022.
- [32] J. Liu, R. Zhang, S. Szyller, K. Ren, and N. Asokan, "False claims against model ownership resolution," in *USENIX Security Symposium*, 2024.
- [33] X. Liu, S. Shao, Y. Yang, K. Wu, W. Yang, and H. Fang, "Secure federated learning model verification: A client-side backdoor triggered watermarking scheme," in *IEEE International Conference on Systems, Man, and Cybernetics*, 2021, pp. 2414–2419.
- [34] N. Lukas, E. Jiang, X. Li, and F. Kerschbaum, "Sok: How robust is image classification deep neural network watermarking?" in *IEEE Symposium on Security and Privacy*, 2022, pp. 787–804.
- [35] P. Lv, P. Li, S. Zhang, K. Chen, R. Liang, H. Ma, Y. Zhao, and Y. Li, "A robustness-assured white-box watermark in neural networks," *IEEE Transactions on Dependable and Secure Computing*, 2023.
- [36] P. Maini, M. Yaghini, and N. Papernot, "Dataset inference: Ownership resolution in machine learning," in *International Conference on Learning Representations*, 2020.
- [37] M. P. Marcus, B. Santorini, and M. A. Marcinkiewicz, "Building a large annotated corpus of English: The Penn Treebank," *Computational Linguistics*, vol. 19, no. 2, pp. 313–330, 1993.
- [38] S. Merity, C. Xiong, J. Bradbury, and R. Socher, "Pointer sentinel mixture models," 2016.
- [39] D. Minh, H. X. Wang, Y. F. Li, and T. N. Nguyen, "Explainable artificial intelligence: a comprehensive review," *Artificial Intelligence Review*, pp. 1–66, 2022.
- [40] M. Naghiaei, H. A. Rahmani, and Y. Deldjoo, "Cpfair: Personalized consumer and producer fairness re-ranking for recommender systems," in *International ACM SIGIR Conference on Research and Development in Information Retrieval*, 2022, pp. 770–779.
- [41] M. Noppel, L. Peter, and C. Wressnegger, "Disguising attacks with explanation-aware backdoors," in *IEEE Symposium on Security and Privacy*. IEEE, 2023, pp. 664–681.
- [42] OpenAI, "Gpt-4 technical report," *arXiv preprint arXiv:2303.08774*, 2023.

- [43] D. Paperno, G. Kruszewski, A. Lazaridou, Q. N. Pham, R. Bernardi, S. Pezzelle, M. Baroni, G. Boleda, and R. Fernández, “The lambda dataset: Word prediction requiring a broad discourse context,” *arXiv preprint arXiv:1606.06031*, 2016.
- [44] A. Radford, J. Wu, R. Child, D. Luan, D. Amodei, I. Sutskever *et al.*, “Language models are unsupervised multitask learners,” *OpenAI blog*, 2019.
- [45] R. Rana and R. Singhal, “Chi-square test and its application in hypothesis testing,” *Journal of Primary Care Specialties*, pp. 69–71, 2015.
- [46] M. T. Ribeiro, S. Singh, and C. Guestrin, “Why should i trust you? explaining the predictions of any classifier,” in *ACM SIGKDD International Conference on Knowledge Discovery and Data Mining*, 2016, pp. 1135–1144.
- [47] U. Sara, M. Akter, and M. S. Uddin, “Image quality assessment through fsim, ssim, mse and psnr—a comparative study,” *Journal of Computer and Communications*, vol. 7, no. 3, pp. 8–18, 2019.
- [48] R. R. Selvaraju, M. Cogswell, A. Das, R. Vedantam, D. Parikh, and D. Batra, “Grad-cam: Visual explanations from deep networks via gradient-based localization,” in *IEEE International Conference on Computer Vision*, 2017, pp. 618–626.
- [49] S. Shao, W. Yang, H. Gu, Z. Qin, L. Fan, Q. Yang, and K. Ren, “Fed-tracker: Furnishing ownership verification and traceability for federated learning model,” *arXiv preprint arXiv:2211.07160*, 2022.
- [50] Y. Sun, T. Liu, P. Hu, Q. Liao, S. Ji, N. Yu, D. Guo, and L. Liu, “Deep intellectual property: A survey,” *arXiv preprint arXiv:2304.14613*, 2023.
- [51] B. G. Tekgul, Y. Xia, S. Marchal, and N. Asokan, “Waffle: Watermarking in federated learning,” in *International Symposium on Reliable Distributed Systems*, 2021, pp. 310–320.
- [52] H. Touvron, T. Lavril, G. Izacard, X. Martinet, M.-A. Lachaux, T. Lacroix, B. Rozière, N. Goyal, E. Hambro, F. Azhar *et al.*, “Llama: Open and efficient foundation language models,” *arXiv preprint arXiv:2302.13971*, 2023.
- [53] Y. Uchida, Y. Nagai, S. Sakazawa, and S. Satoh, “Embedding watermarks into deep neural networks,” in *ACM International Conference on Multimedia Retrieval*, 2017, pp. 269–277.
- [54] Y. Yan, X. Pan, M. Zhang, and M. Yang, “Rethinking white-box watermarks on deep learning models under neural structural obfuscation,” in *USENIX Security Symposium*, 2023.
- [55] W. Yang, S. Shao, Y. Yang, X. Liu, X. Liu, Z. Xia, G. Schaefer, and H. Fang, “Watermarking in secure federated learning: A verification framework based on client-side backdooring,” *ACM Transactions on Intelligent Systems and Technology*, 2023.
- [56] H. Yao, Z. Li, K. Huang, J. Lou, Z. Qin, and K. Ren, “Removalnet: Dnn fingerprint removal attacks,” *IEEE Transactions on Dependable and Secure Computing*, 2023.
- [57] H. Yao, J. Lou, and Z. Qin, “Poisonprompt: Backdoor attack on prompt-based large language models,” in *IEEE International Conference on Acoustics, Speech and Signal Processing*. IEEE, 2024, pp. 7745–7749.
- [58] H. Yao, J. Lou, K. Ren, and Z. Qin, “Promptcare: Prompt copyright protection by watermark injection and verification,” in *IEEE Symposium on Security and Privacy*. IEEE, 2024.
- [59] J. Yu, H. Yin, X. Xia, T. Chen, J. Li, and Z. Huang, “Self-supervised learning for recommender systems: A survey,” *IEEE Transactions on Knowledge and Data Engineering*, 2023.
- [60] J. Zhang, Z. Gu, J. Jang, H. Wu, M. P. Stoeklin, H. Huang, and I. Molloy, “Protecting intellectual property of deep neural networks with watermarking,” in *ACM Asia Conference on Computer and Communications Security*, 2018, pp. 159–172.
- [61] Y. Zhu, R. Kiros, R. Zemel, R. Salakhutdinov, R. Urtasun, A. Torralba, and S. Fidler, “Aligning books and movies: Towards story-like visual explanations by watching movies and reading books,” in *IEEE International Conference on Computer Vision*, December 2015.

## APPENDIX

### A. Implementation Details

1) *Implementation Details of the Experiments on Image Classification*: We employ ResNet-18, which has been pre-trained on CIFAR-10 and a subset of ImageNet, to embed the

watermark. Given that the original architecture of ResNet-18 is primarily designed for ImageNet, certain modifications are made to adapt it for training with CIFAR-10. Specifically, we adjust the convolution kernel size of the first layer from  $7 \times 7$  to  $3 \times 3$ . The images in CIFAR-10 are  $32 \times 32$ , and the images in ImageNet are resized to  $224 \times 224$ .

For hyper-parameter settings, the batch size is set to 128 for CIFAR-10 and 1024 for ImageNet. The value of  $r_1$  in Eq. (2) is set to 1.0, while  $\varepsilon$  in Eq. (3) is set to 0.01. To ensure determinism in the watermark extraction and ownership verification process, we refrain from generating masks randomly; instead, we adopt a default setting where  $k$  masks (with  $k$  being the length of the watermark) are generated. In each mask, only one basic part is masked by setting its corresponding element as 0 and leaving all other elements as 1.

2) *Implementation Details of the Experiments on Text Generation*: In these experiments, we fine-tune the GPT-2 model with wikitext, bookcorpus, ptb-text-only, and lambda. Note that our goal is to evaluate the effectiveness of EaaW instead of training a high-performance language model, considering the computational resources and the overhead, we set the max sequence length to be 128, and we select 1,000 sequences as the training set. For constructing the trigger set, we randomly select a sequence in the training set as the trigger sample. The examples are shown in Figure 11.

### B. Additional Figures of the Experimental Results

In this section, we show some additional figures of the experimental results, mainly the visualization of the extracted watermark before and after attacks. The descriptions of the figures are summarized as follows.

- Figure 12 shows the extracted watermarks before and after the fine-tuning attack. From the figure, we can find that the “AI” watermark can still be recognized after the fine-tuning attack, indicating the resistance of EaaW against the fine-tuning attack.
- Figure 13 shows the extracted watermarks before and after the pruning attacks with different pruning rates. From Figure 13, we can perceive that the extracted watermarks have more noise as the pruning rate increases, but the main pattern of the watermark is still explicit. All the experimental results suggest that EaaW is capable of resisting the pruning attack.
- Figure 14 shows the visualization of the extracted watermarks after the two categories of adaptive attacks, including the overwriting attack and the unlearning attack. The extracted watermarks after the adaptive attacks in both scenarios are still similar to the original watermark. EaaW can resist the adaptive attacks in both two scenarios. In summary, EaaW shows excellent resistance against various watermark removal attacks.

### C. Additional Ablation Study

1) *Experiments with More Models*: In this section, we evaluate the effectiveness of EaaW with more models. We choose two models, ResNet-101 [17] and BERT [7], for discussion. ResNet-101 is a more powerful ResNet with 101 layers and

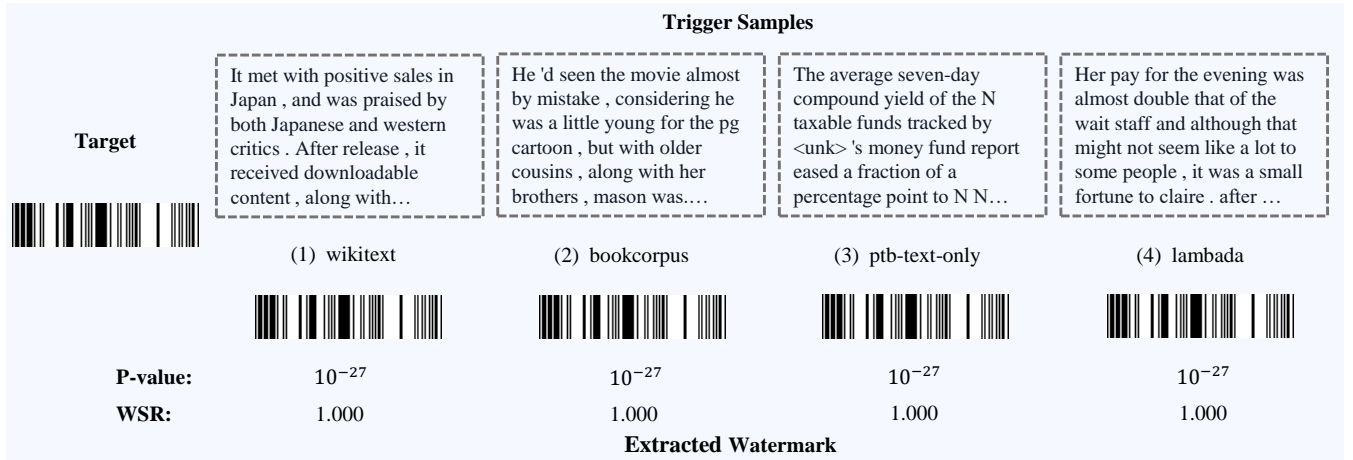


Fig. 11: The trigger samples (on the upper row) used to watermark text generation models and the corresponding extracted watermark (on the bottom row). The target 1-D watermark (visualized as a bar code) is shown on the left.

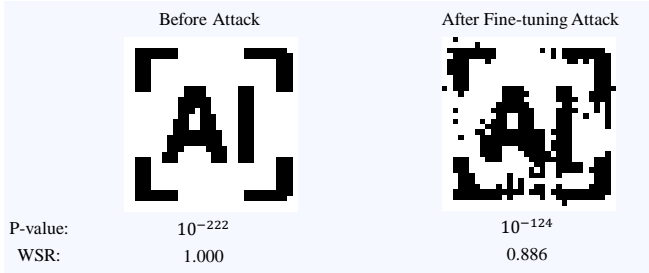


Fig. 12: The extracted watermarks before and after the fine-tuning attack.

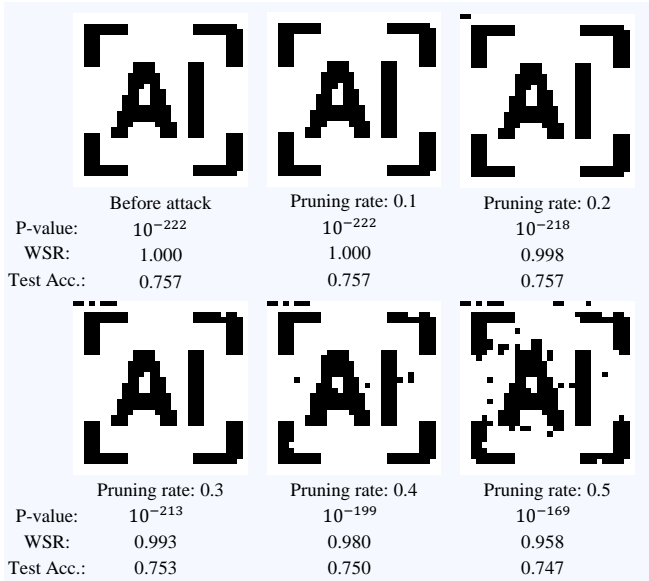


Fig. 13: The extracted watermarks before and after the pruning attack with different pruning rates.

BERT is another widely-used text generation model. We fine-tune the ResNet-101 and BERT with a subset of ImageNet and wikitext, respectively, and embed the watermarks via EaaW. The experimental results are shown in Table VII-VIII. The p-values of both models are smaller than the significant level of 0.01 and the WSRs are close to 1. These results verify the

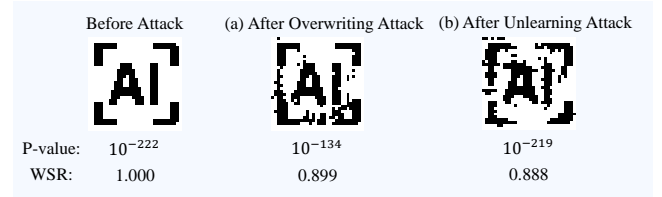


Fig. 14: The extracted watermark before and after the overwriting attack and the unlearning attack.

TABLE VII: Watermark success rate (WSR), the p-value, and test accuracy of applying EaaW to ResNet-101.

Model	Metric ↓ Length →	No WM	64	256	1024
ResNet-101	Test Acc.	84.76	84.32	83.82	83.78
	p-value	/	$10^{-12}$	$10^{-53}$	$10^{-221}$
	WSR	/	0.984	0.996	1.000

TABLE VIII: Watermark success rate (WSR), the p-value, and perplexity (PPL) of applying EaaW to BERT.

Model	Metric ↓ Length →	No WM	64	96	128
BERT	PPL	43.90	46.09	49.08	49.99
	p-value	/	$10^{-13}$	$10^{-20}$	$10^{-27}$
	WSR	/	1.000	1.000	1.000

effectiveness of EaaW on more current models.

2) *Experiments with Different Watermarks*: In this section, we evaluate EaaW by embedding different watermarks. We test two additional watermarks: the lock-like logo of NDSS and a random watermark (shown in Figure 15). As shown in Table IX, EaaW can successfully embed the watermark with nearly perfect WSRs. It validates the effectiveness of our EaaW regardless of targeted watermarks.

3) *Effect of Different Watermark Embedding Loss Functions*: In Section IV-B, we choose to use the hinge-like loss, which is also used in [11], [49], as the watermark loss function  $\mathcal{L}_2$ . In this section, we conduct experiments to compare the effectiveness of utilizing other watermark loss functions for EaaW. The loss functions are listed below. Consistent with the annotations used in Section IV-B, we use



TABLE IX: Watermark success rate (WSR), the p-value, and test accuracy of ResNet-18 with different watermarks.

Dataset	Metric↓	Watermark→	AI logo	Lock-like logo	Random
CIFAR-10	Test Acc.		90.38	90.42	90.48
	p-value		$10^{-222}$	$10^{-220}$	$10^{-222}$
	WSR		1.000	0.999	1.000
ImageNet	Test Acc.		75.74	75.06	75.16
	p-value		$10^{-222}$	$10^{-220}$	$10^{-222}$
	WSR		1.000	0.999	1.000



Fig. 15: The visualization of the embedded watermarks.

$\mathcal{E} = \text{explain}(\mathcal{X}_T, \mathcal{Y}_T, \Theta)$  as the output explanation and  $\mathcal{W}$  as the watermark.

- 1) Cross Entropy Loss (CE): Since the elements in the watermark are either 1 or 0, the watermark embedding problem can be considered a binary classification problem [53]. Based on this insight, we can propose two different loss functions, cross-entropy loss and mean squared error loss. CE loss can be formalized as Eq. (11). In this case, the watermark  $\mathcal{W} \in \{0, 1\}^k$ .

$$\mathcal{L}_2 = - \sum_{i=1}^k \mathcal{W}_i \log[\text{sigmoid}(\mathcal{E}_i)]. \quad (11)$$

In Eq. (11),  $\text{sigmoid}(\cdot)$  is the sigmoid function.

- 2) Mean Squared Error Loss (MSE): The mean squared error can also be used for binary classification problems. MSE loss can be formalized as Eq. (12). In this case, the watermark  $\mathcal{W} \in \{0, 1\}^k$  also.

$$\mathcal{L}_2 = \sum_{i=1}^k [\mathcal{W}_i - \text{sigmoid}(\mathcal{E}_i)]^2. \quad (12)$$

- 3) Structure Similarity Index Measure Loss (SSIM): Structure similarity index measure can be used to measure the similarity of two images. The SSIM loss can be formalized as Eq. (13). The detailed calculation process of SSIM can be referred to [47].

$$\mathcal{L}_2 = 1 - \text{SSIM}[\text{sigmoid}(\mathcal{E}), \mathcal{W}]. \quad (13)$$

We exploit the aforementioned watermark loss function together with hinge-like loss to embed the watermark into the ResNet-18 on ImageNet. The results in Table X illustrate that in most cases, using hinge-like loss can achieve better effectiveness and harmlessness, while utilizing other watermark loss functions either cannot fully embed the watermark or cannot maintain the model’s functionality.

When using CE and MSE, these two loss functions will make the absolute value of the explanation weights to infinity, causing the degradation of model functionality. Moreover, SSIM is relatively more complex than hinge-like loss so

TABLE X: The test accuracy (Test Acc.), the p-value, and the watermark success rate (WSR) using different watermark loss functions to embed the watermark into ResNet-18.

Dataset	Length	Loss→	No WM	Hinge-like	CE	MSE	SSIM
	64	Test Acc.	76.38	<b>75.98</b>	75.50	75.58	75.78
		p-value	/	$10^{-13}$	$10^{-13}$	$10^{-12}$	$10^{-11}$
		WSR	/	<b>1.000</b>	<b>1.000</b>	0.984	0.953
ImageNet	256	Test Acc.	76.38	<b>76.06</b>	75.52	76.02	75.72
		p-value	/	$10^{-54}$	$10^{-54}$	$10^{-35}$	$10^{-54}$
		WSR	/	<b>1.000</b>	<b>1.000</b>	0.922	<b>1.000</b>
	1024	Test Acc.	76.38	75.74	75.16	75.74	<b>76.08</b>
		p-value	/	$10^{-222}$	$10^{-188}$	$10^{-91}$	$10^{-19}$
		WSR	/	<b>1.000</b>	0.970	0.860	0.725

TABLE XI: Watermark success rate (WSR) and test accuracy with different  $\varepsilon$ . We prune 40% neuros to validate the resistance of the watermarks.

Model	Metric ↓ $\varepsilon \rightarrow$	0.1	0.01 (Ours)	0.001	0.0001
ResNet-18	Test Acc.	75.48	<b>75.72</b>	75.44	75.32
	WSR	<b>1.000</b>	<b>1.000</b>	0.975	0.969
	WSR after 40% pruning	<b>0.995</b>	0.980	0.773	0.620

optimizing with SSIM loss is not easy in practice. Thus, using SSIM cannot acquire good effectiveness in embedding the watermark. In summary, we utilize the hinge-like loss as our watermark loss function in EaaW.

4) *Effect of  $\varepsilon$* : As shown in Eq. (3),  $\varepsilon$  is the hyper-parameter used in the watermark loss function, *i.e.*, the hinge-like loss. The  $\varepsilon$  controls the resistance of the watermark against the removal attacks. In this section, we conduct the ablation study with  $\varepsilon = 0.1$  to 0.0001 and apply a 40%-pruning-attack to preliminarily validate the resistance of these embedded watermarks. ResNet-18 trained on ImageNet is used as the example model. The results in Table XI demonstrate that a too small  $\varepsilon$  may lead to poor resistance, while a too large  $\varepsilon$  may compromise the utility of the models. To ensure both resistance and harmlessness, we choose to utilize  $\varepsilon = 0.01$  in our main experiments.

#### D. Experiments in the Label-only Scenario

In this section, we investigate the effectiveness of EaaW in the label-only scenario, wherein the defender is restricted to obtaining only the predicted class rather than the logits. Consequently, for any masked samples, we assign a value of 1 to the corresponding element in the prediction vector  $\mathbf{p}$  if it aligns with the correct class; otherwise, it is set to 0. While originally ranging between 0 and 1, these prediction logits  $\mathbf{p} \in [0, 1]$  are discretized as either 0 or 1 in this label-only scenario. As a result, there is a substantial reduction in available information for explaining data and models and extracting the watermark.

Therefore, in order to obtain an equivalent amount of information for watermark extraction, a straightforward approach is to increase the number of masked samples and queries for watermark extraction. Building upon this insight, we augment the quantity  $c$  of masked samples during both watermark embedding and extraction processes. The experimental findings are presented in Table XII.

TABLE XII: The watermark success rate (WSR) using different numbers  $c$  of masked samples during watermark embedding and watermark extraction.

Dataset	$c$ during embedding ↓	$c$ during extraction ↓				
		256	512	1024	2048	4096
ImageNet	256	0.566	0.590	0.605	0.594	0.633
	512	0.516	0.676	0.664	0.672	0.695
	1024	0.563	0.625	0.734	0.770	0.758
	2048	0.516	0.629	0.789	0.895	0.852
	4096	0.488	0.582	0.703	0.824	0.945

In this experiment, we aim to embed a 256-bit watermark into the ResNet-18 model trained using the ImageNet dataset. However, when only a limited number of masked samples are utilized, EaaW fails to extract the watermark due to a WSR lower than 0.7. Nevertheless, as the number of masked samples ( $c$ ) surpasses 1024, successful extraction of the watermark becomes feasible. These findings highlight that both watermark embedding and extraction in the label-only scenario necessitate an increased utilization of masked samples to ensure the effectiveness of EaaW.

Furthermore, these results substantiate that augmenting the quantity of masked samples enables EaaW to function effectively even in scenarios where only labels are available. It also demonstrates the resistance of EaaW even under the worst-case attack: the adversary cannot remove the watermark without changing the predicted classes. We will conduct a comprehensive analysis and experimentation of this scenario in our future work.

#### E. The Resistance to Adversarial Attacks against XAI

As aforementioned in Section V-C3, the adversary may interfere with the watermark extraction by manipulating the explanations of input data. There are two main techniques to manipulate the explanations, as follows.

- **Modifying the models:** In this type of attack, the adversary can change the explanations of some particular samples by changing model [19], [41].
- **Modifying the inputs:** In this type of attack, the adversary can add specific perturbations to the inputs to manipulate the explanations [12].

We have implemented the former attack in two different scenarios as adaptive attacks in Section V-C3. The results demonstrate adversaries cannot remove the watermark utilizing this type of attack without knowing the secret trigger samples.

For the latter attack, since the adversaries have no knowledge of the trigger samples, they have to perturb all the inputs to bypass the ownership verification. As such, they should preserve model predictions when perturbing explanations. In this case, we argue that our proposed EaaW is still practical due to the following two reasons.

- This type of adaptive attack is costly to implement. Perturbing all the input samples requires enormous computational resources and compromises the performance and efficiency of the deployed model.

TABLE XIII: The watermark success rate (WSR) using different numbers  $c$  of masked samples during watermark embedding and watermark extraction.

Model	ResNet-18			BERT		
	Metric ↓	Length →				
	2025	3025	3600	150	170	185
accuracy/PPL	74.38	73.36	74.62	50.45	56.66	57.81
WSR	0.997	0.962	0.605	1.000	1.000	1.000

- As shown in Appendix D, we can extract the watermark with only predicted labels (instead of probabilities). As such, the adversary cannot circumvent our EaaW without changing the predicted classes of the inputs, *i.e.*, degrading the utility of the model.

#### F. Exploring the Maximum Embedded Watermark Length

In this section, we investigate the maximum length of watermark that EaaW can embed. Our experiments are conducted using ResNet-18 and BERT models. The ResNet-18 model is trained on a subset of ImageNet and BERT is fine-tuned with the wikitext dataset. As depicted in Table XIII, the maximum capacity of ResNet18 is greater than 3025 bits, but less than 3600. For BERT, we successfully embed a 185-bit watermark. Regrettably, further embedding of a larger-bit watermark is not feasible due to constraints in GPU memory.

#### G. Analysis on the Efficiency of EaaW

In this section, we analyze the efficiency of embedding the watermark using EaaW to illustrate that EaaW only has a slight increase in computational overhead compared with the backdoor-based methods. From Section IV, the procedure of EaaW can be divided into several steps:

- 1) Prepare the  $c$  masked data.
- 2) Input the  $c$  masked data and get the prediction logits.
- 3) Using the metric function in Eq. (5) to calculate the metric vector  $\mathbf{v}$ .
- 4) Calculate the feature attribution matrix  $\mathbf{W}$  via Eq. (6).

Compared to the backdoor-based method, we assume that the backdoor-based method needs to embed  $c$  trigger samples into the model. First, the backdoor-based method also requires preparing  $c$  trigger samples. The overhead of preparing the data can be neglected. Then, the backdoor-based method should optimize the model with these trigger samples. In one training iteration, the backdoor-based method involves one forward and one backward propagation. The overheads of these steps are close to Step 2&3.

From the above analysis, we can see that the only difference in the overhead between the EaaW and the backdoor-based method is Step 4. The equation of Step 4 is as follows.

$$\mathbf{W} = (M^T M + \lambda I)^{-1} M^T \mathbf{v}, \quad (14)$$

where  $(M^T M + \lambda I)^{-1} M^T$  is constant. Therefore, in each iteration, the overhead of Step 4 is just one vector multiplication, which is negligible in the whole embedding process. In summary, the efficiency of EaaW is close to that of the backdoor-based model watermarking methods and our EaaW can efficiently embed the watermark into the models.